EFFECT OF ANGULAR ORIENTATION ON THE HYDRODYNAMIC FORCES ACTING ON A BODY IN A RESTRICTED WATERWAY

by

Jared Lawrence Wells

Thesis submitted to the Faculty of the
Virginia Polytechnic Institute and State University
in partial fulfillment of the requirements for the degree of
Master of Science
in
Aerospace and Ocean Engineering

APPROVED:

Dr. Paul Kaplan, Chairman

Dr. Bernard Grossman

Dr. Wayne Neu

December, 1985

Blacksburg, Virginia

EFFECT OF ANGULAR ORIENTATION ON THE HYDRODYNAMIC FORCES ACTING ON A BODY IN A RESTRICTED WATERWAY

by

Jared Lawrence Wells

Dr. Paul Kaplan, Chairman

Aerospace and Ocean Engineering

(ABSTRACT)

A slender body theory method developed for a body moving parallel to a wall in shallow water is extended to include angular orientation of the body to the wall. The method satisfies only the zero normal velocity condition on the external boundaries but does not take into account the effect of induced flows on the body itself. A spheroid and a Series 60, block .80 hull were the bodies studied. The side force and yaw moment on each body were determined numerically for varying angular orientation with respect to either a single wall or canal bank. For both cases results for a range of depths and wall separation distances are presented. It is found that the method gives good qualitative side force predictions for a body moving parallel to a wall, but is unable to correctly predict the yaw moment or the side force due to angular orientation. This result dictates the need for a more complex mathematical model to properly represent

the flow than the simple model and quasi-steady method used here.

ACKNOWLEDGEMENTS

I would like to extend my thanks to the following people for their direct and indirect contributions to this thesis.

Dr. Kaplan for serving as my committee chairman.

Dr. Grossman and Dr. Neu for serving on my committee.

The students and faculty at Virginia Tech, especially Dr. Moore, Dr. Schetz, Dr. Grossman, and Professor Williams, for enriching this educational experience.

for their friendship and ideas.

for their bicycling companionship.

Others here unnamed in both the Aerospace and Mechanical Engineering Departments for their friendship.

My parents, my brothers and and my new family the for their love and encouragement.

And for everything.

TABLE OF CONTENTS

LIST OF ILLUSTRATIONS

NOMENCLATURE

D ..... Body diameter (hull plus reflection)

$f(x)$ ..... Source strength per unit length

g ..... Gravitational constant

h ..... Fluid depth

ℓ ..... $\frac{1}{2}L$

L ..... Body length

m_1 ..... Source strength internal to the stream surface

N ..... Yaw moment

N'' ..... Nondimensional yaw moment, 'bis' system

q_y ..... Resultant y direction fluid velocity at the location of the original source distribution due to all other sources

r,θ,x ..... Cylindrical coordinate system

R ..... Body of revolution radius

S ..... Cross sectional area

$S'(x)$ ..... Derivative of the cross sectional area with respect to x

u_r ..... Velocity in the r-axis direction

u'' ..... Froude number, 'bis' system

U ..... Constant forward velocity

w ..... Canal width

x,y,z ..... Cartesian coordinate system

x_1,y_1,z_1 ... Rotated cartesian coordinate system

y_o ..... Distance from body center to canal centerline

y_s ..... Distance from body center to wall

Y ..... Side force normal to the body

Y'' ..... Nondimensional side force, 'bis' system

β ..... Angle between x-axis and x_1-axis

ξ ..... Dummy variable

ξ_1 ..... Dummy variable

ρ ..... Mass density of the fluid

ϕ ..... Velocity potential

∇_o ..... Volume displacement at rest

∇ ..... Del operator

∂ ..... Partial derivative

1.0 INTRODUCTION

1.1 BACKGROUND

The motion of ships in restricted waters continues to be a problem of major interest in naval hydrodynamics. In recent years, ships have increased in size causing the waterways to become even more restrictive. In these confined waters, the hydrodynamic forces and moments tend to differ considerably from those experienced in open water. This variation gives rise to situations in which collisions may occur with either a stationary object or another ship. Experimental data for these situations is often hard to obtain. It is therefore desirable to develop a theoretical method to predict these forces and moments.

One area of focus involves the hydrodynamic interactions of a ship in a channel or a ship in shallow water approaching a bank. In most real situations, these banks or channels would have sloping sides and an uneven bottom. Shoaling can also be present. These obstacles are hard to model, and generally most theoretical methods make major simplifications. As a result, the banks and bottom are often modeled as vertical and horizontal planes respectively [2,7,11].

1.2 SCOPE OF WORK

The purpose of this study was to take a simple theoretical method derived for a ship moving parallel to a vertical wall in shallow water, and test its capability to be extended into other situations. The method that was used was a 3-D analysis developed by Newman [11]. Newman derived a slender body theory model by establishing the velocity potential for a body of revolution in an infinite fluid and introducing the effect of nearby boundaries. These boundaries consisted of two vertical walls parallel to the body axis and a horizontal bottom. The method of images was used to satisfy the zero normal velocity condition on the boundaries. No additional singularities were added to correct the body alterations that were due to the cross flow generated by the images. This procedure of satisfying only the zero normal velocity condition on the external boundaries, and not on the body itself represents a first basic step of analysis that has been applied in various free surface problems [10]. With this method, Newman investigated the bank suction forces acting on a spheroid running parallel to either a single wall or a canal bank.

The capability of this theory to predict side force and yaw moment for angular orientation relative to the wall was the application considered in this thesis. This is an extension of the analysis done by Newman to include the effects

of angular orientation, as well as including an investigation of the yaw moment. Along with evaluating the extended method for a spheroid, a realistic ship form will be studied. The effects of water depth and distance from the near wall will also be investigated. Of interest was the ability of a simple quasi-static method, which was an extension of the basic analysis by Newman, to predict the hydrodynamic forces for the particular case of a ship approaching a wall at a given angle.

The major assumptions made in the 3-D slender body theory model presented here include:

- The fluid is an ideal fluid.
- The Froude number is small.
- In the cases of angular orientation
  1. The angles will be relatively small, less than 25°.
  2. The unsteadiness of the body approaching the wall is neglected. The problem is evaluated at a particular instant.
- No singularities are added to correct body alterations.
- Separation distances are greater then a body diameter.
- Twice the submerged cross sectional area of a realistic ship form may be taken as an equivalent body of revolution [11].

This thesis starts with the development of the velocity potential for a slender body in an unbounded fluid. Side force and yaw moment expressions are then developed for specific boundary conditions. After a brief description of the

computation procedure, numerical results are presented graphically. Two computer programs are included as references.

1.3 LITERATURE REVIEW

Although a variety of literature exists on the subject of restricted waterways, a limited number of papers were found that had bearing on the specific problem examined in this work. Of these, only two papers discuss the problem of angular orientation. Hess [7] dealt with the 2-D unsteady hydrodynamic interactions of a ship approaching a vertical wall at an oblique angle. He considered the ship as a slender body with a trailing edge, taking into account crossflow and blockage. Hess found that the side force and yaw moment increase with decreasing water depth and/or decreasing wall separation distance. The yaw moment was found to be always bow away from wall. He claims that increasing angle decreases the resultant side force.

Dand [6] ran a series of model experiments in a shallow channel. Here he showed that a vessel approaching a bank at an angle usually experienced a bank rejection phenomena. Calculations made using a steady state 2-D source panel method including circulation showed that for an angle of 20° to 40°, the ship experienced a bank rejection moment. Side force calculated by the same method indicated a bank re-

jection for a 20° to 60° angle, but had the expected bank suction for motion parallel to the bank.

Newman [11], whose method is the basis for this current work, used slender body theory with the method of images. He produced numerical results for a spheroid moving with constant velocity parallel to either a single wall or canal bank. From the results it is evident that the side force increases monotonically when the body is increasingly far away from the centerline of the canal, but at a rate that depends on both the width and depth. For the single wall it is shown that the side force decreases for an increasing separation distance, again at a rate which is dependent upon the depth. Both cases show the side force as a bank suction force.

Beck [2] calculated the side force and yaw moment acting on a slender ship traveling with a constant velocity parallel to the centerline of a rectangular canal by the method of matched asymptotic expansions. His results show a bank suction force, which he claims is greatly affected by the crossflow under the ship (which he takes into account). The crossflow also reverses the direction of the yaw moment, resulting in the proper bow away from wall moment. These results are generally corroborated qualitatively by experimental data.

Recently, Cohen and Beck [4] conducted model tests for a simple mathematically defined hull in order to compare with

linearized theories. The results showed a bank suction force and a bow away from wall moment for both the experimental data and theoretical predictions. They concluded that the linearized theory they outlined gave reasonable predictions as to the hydrodynamic interactions encountered.

2.0 ANALYSIS

The problem considered was that of a body moving with a constant velocity U in proximity to a single wall or within a canal. A right-hand Cartesian coordinate system (x,y,z) is used. The z-axis points vertically downward, with z=0 the plane of the undisturbed free surface. The x-axis is positive forward, and the y-axis is to starboard with y=0 the plane of the centerline of either the body or of the canal. The origin of the coordinate system is at amidships, so that the body lies along the x-axis occupying the region between x= +½L (bow) and x= -½L (stern), where L is the body length. The wall or walls are taken as vertical planes parallel to the z-axis, and the bottom is considered to be a horizontal plane. It is assumed that the transverse dimensions of the body are small compared to the length of the body.

For sufficiently small Froude numbers, the free surface may be considered to be effectively equivalent to a horizontal plane rigid wall boundary. This allows, by the method of images, the flow past the submerged portion of the hull to be equal to one-half the flow past the submerged hull plus its reflection above the free surface in a fluid unbounded in the vertical extent. Thus a double body is created at the free surface which will be considered as a body of revolution. The assumption will then be made that twice the

submerged hull of a realistic ship form may be considered to be an equivalent body of revolution [1,11]. This assumption is reasonable due to the fact that the ship (in this case a Series 60, block .80 hull) is generally symmetric about the longitudinal axis, and has a smooth variation of cross section along the longitudinal axis. This can be seen in Figure 6 in Chapter 3.

For a body of revolution the body surface can be described by the equation r=R(x), where R is the body radius, using the cylindrical coordinate system (r,θ,x) as shown in Figure 1. The mathematical problem for axisymmetric flow past a slender body of revolution in an unbounded ideal fluid may then be defined as follows [8]:

$$\phi=\phi(r,x)$$

$$\nabla^2\phi = \frac{\partial^2\phi}{\partial r^2} + \frac{1}{r}\frac{\partial\phi}{\partial r} + \frac{\partial^2\phi}{\partial x^2} = 0 \qquad (1)$$

$$\frac{\partial\phi}{\partial r}(R,x) = u_r(R,x) = U\frac{dR}{dx} \qquad -\ell \le x \le \ell \qquad (2)$$

where $\nabla\phi=0$ at infinity and $\ell = \frac{1}{2}L$.

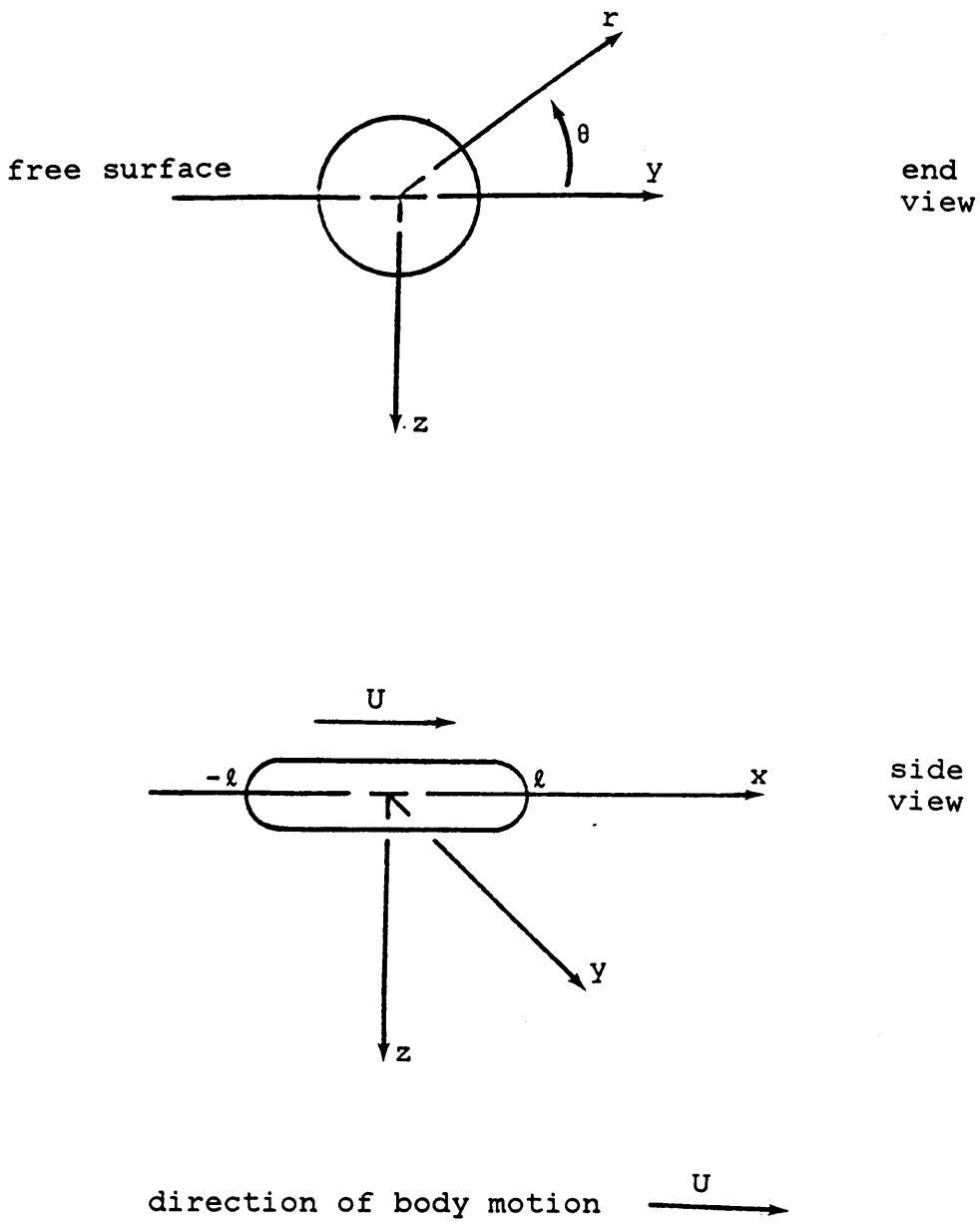

Figure 1. Cylindrical Coordinate System.

The basic potential solution to this problem may be represented by a distribution of sources along the x-axis, with the potential given by

$$\phi(x,r) = -\int_{-\ell}^{\ell} \frac{f(\xi)\, d\xi}{[(x-\xi)^2+r^2]^{\frac{1}{2}}} \tag{3}$$

where $f(\xi)$ is the source strength per unit length.

The source strength per unit length ($f(\xi)$) is determined by satisfying the boundary conditions. To examine an approximate form of the boundary conditions for slender bodies, the governing equation will be investigated. Equation (1) may be rewritten as

$$\frac{1}{r}\frac{\partial}{\partial r}\left(r\frac{\partial \phi}{\partial r}\right) + \frac{\partial^2 \phi}{\partial x^2} = 0$$

Since $\frac{\partial^2 \phi}{\partial x^2}$ is bounded

$$r\frac{\partial^2 \phi}{\partial x^2} \to 0 \quad \text{as} \quad r \to 0$$

therefore $\left(\frac{\partial \phi}{\partial r} = u_r\right)$

$$\frac{\partial}{\partial r}(ru_r) \to 0 \quad \text{as} \quad r \to 0$$

so that near the axis, ru_r is a function of x. Thus, for small values of r, u_r is singular

$$u_r \sim 1/r$$

However the combination of ru_r is well behaved and may be expanded in a Maclaurin series about r=0. The approximate slender body form of the boundary condition (2) becomes [9]

$$(ru_r)_{r=0} = UR\frac{dR}{dx} \tag{4}$$

The left hand side of the boundary condition, $(ru_r)_{r=0}$, can be approximated by using equation (3), and evaluating as $r \to 0$. This is seen as follows

$$\lim_{r\to 0}(ru_r) = \lim_{r\to 0} \int_{-\ell}^{\ell} \frac{r^2 f(\xi)\, d\xi}{[(x-\xi)^2+r^2]^{3/2}} = UR\frac{dR}{dx}$$

Therefore [8]

$$2f(x) = UR\frac{dR}{dx} \tag{5}$$

The cross sectional area S of the body may be described by $S=\pi R^2$. Therefore

$$\frac{dS}{dx} = 2\pi R\frac{dR}{dx}$$

or

$$\frac{S'(x)}{2\pi} = R\frac{dR}{dx} \tag{6}$$

Combining equations (5) and (6)

$$2f(x) = U \frac{S'(x)}{2\pi}$$

or

$$f(x) = \frac{U}{4\pi} S'(x) \tag{7}$$

Thus by equations (3) and (7), and $r^2 = y^2 + z^2$, the solution in Cartesian coordinates to the mathematical problem posed is

$$\phi(x,y,z) = \frac{-U}{4\pi} \int_{-\ell}^{\ell} \frac{S'(\xi)\, d\xi}{[(x-\xi)^2+y^2+z^2]^{\frac{1}{2}}} \tag{8}$$

Although equation (8) has been derived for a slender body of revolution, it will be assumed valid for any general slender body [11]. At a sufficient separation distance, this assumption is in agreement with the equivalence rule which states "Far away from a general slender body the flow becomes axisymmetric and equal to the flow around the equivalent body of revolution." [1].

2.1 SIDE FORCE AND YAW MOMENT FOR A SINGLE WALL

2.1.1 BODY PARALLEL TO THE WALL

The velocity potential solution for the unbounded fluid may then be corrected for specific boundary conditions. First, a body running parallel at a distance $y=y_s$ from a single vertical wall in a fluid depth of z=h will be examined (see Figure 2). To satisfy the zero velocity condition on the wall, an image source distribution was located at $y=2y_s$. Since the body is really a submerged hull plus its reflection, the presence of the bottom below the hull will cause each half of the body to 'see a bottom' at a distance h. An image source distribution located at z=2h will satisfy the zero normal velocity condition on the 'bottom' located at z=h. However, the source distribution at z=2h will then have an unsatisfied flow at the 'bottom' located at z= -h. The condition here may be satisfied by locating another source distribution at z= -4h. By the same reasoning, the source distribution at z= -2h needs a source distribution at z=4h. These new source distributions then need their flow on the 'bottoms' satisfied, and the process continues onward. The result is a cascade of source distributions in the vertical direction located at z=2mh where m takes on all integer values between $\pm\infty$.

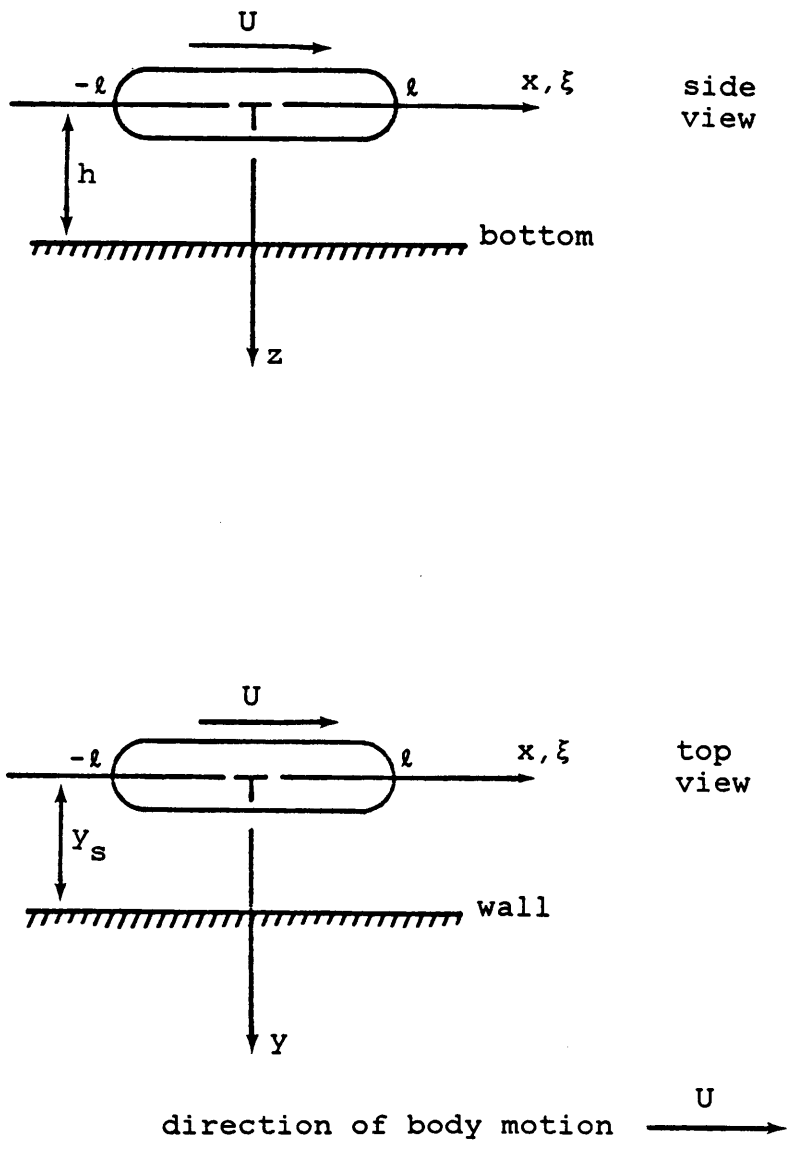

Figure 2. Coordinate System for a Body Parallel to a Single Wall.

The velocity potential in equation (8) then may be written as

$$\phi(x,y,z) = \frac{-U}{4\pi} \sum_{m=-\infty}^{\infty} \int_{-\ell}^{\ell} S'(\xi)[(x-\xi)^2+y^2+(z-2mh)^2]^{-\frac{1}{2}}d\xi \qquad (9)$$

$$- \frac{U}{4\pi} \sum_{m=-\infty}^{\infty} \int_{-\ell}^{\ell} S'(\xi)[(x-\xi)^2+(y-2y_s)^2+(z-2mh)^2]^{-\frac{1}{2}}d\xi$$

where the first term represents the body and its reflections in the vertical plane, and the second term represents the horizontal image plus its reflections in the vertical plane.

The steady side force Y can be determined by Lagally's theorem [5]

$$Y = -4\pi\rho f(x)q_y \qquad (10)$$

where

- $f(x)$ is the source strength per unit length internal to the stream surface
- q_y is the resultant y direction fluid velocity at the location of the original source distribution due to all other sources
- ρ is the mass density of the fluid

The resultant fluid velocity in the y direction may be determined by taking the partial derivative of equation (9) with respect to y, and when evaluated at the original source distribution where x=x, y=0, and z=0, then

$$q_y = \frac{-U}{4\pi} \sum_{m=-\infty}^{\infty} \int_{-\ell}^{\ell} 2y_s S'(\xi)[(x-\xi)^2+4y_s^2+4m^2h^2]^{-3/2} d\xi$$

From equation (7), $f(x)=US'(x)/(4\pi)$. Therefore from equation (10), the side force on the body is

$$Y = \frac{\rho U^2}{4\pi} \sum_{m=-\infty}^{\infty} \int_{-\ell}^{\ell} S'(x) \int_{-\ell}^{\ell} 2y_s S'(\xi)[(x-\xi)^2+4y_s^2+4m^2h^2]^{-3/2} d\xi dx \quad (11)$$

which agrees with Newman's [11] result.

The resultant yaw moment about the z-axis is [5]

$$N = \frac{\rho U^2}{4\pi} \sum_{m=-\infty}^{\infty} \int_{-\ell}^{\ell} xS'(x) \int_{-\ell}^{\ell} 2y_s S'(\xi)[(x-\xi)^2+4y_s^2+4m^2h^2]^{-3/2} d\xi dx \quad (12)$$

2.1.2 BODY AT AN ANGLE TO THE WALL

The problem of a body with angular orientation β to a single vertical wall in shallow water is very similar to that of a body parallel to a single wall in shallow water. The unsteady effect of the body approaching the wall will be neglected and an instantaneous snapshot is considered. A rotated coordinate system is aligned with the body axis. The x_1-axis is positive forward, and makes an angle β with the x-axis. The z_1-axis is down and the y_1-axis completes the right handed coordinate system as shown in Figure 3. The

origin is at the body center in water of depth h, and the wall is at a distance of y_s from the body center. The zero velocity condition on the wall will be satisfied by an image source distribution at $y=2y_s-\xi_1\sin\beta$, where $-\ell \le \xi_1 \le \ell$. As in the previous case, a cascade of source distributions will be located at $z=2mh$ where m takes on all integer values between $\pm\infty$.

The velocity potential in equation (8) may then be written for a body with angular orientation to a single wall in shallow water as

$$\phi(x,y,z) = \frac{-U}{4\pi} \sum_{m=-\infty}^{\infty} \int_{-\ell}^{\ell} \{S'(\xi_1) \times [(x-\xi_1\cos\beta)^2+(y-\xi_1\sin\beta)^2+(z-2mh)^2]^{-\frac{1}{2}}\} d\xi_1$$

$$- \frac{U}{4\pi} \sum_{m=-\infty}^{\infty} \int_{-\ell}^{\ell} \{S'(\xi_1) \times [(x-\xi_1\cos\beta)^2+(y-2y_s+\xi_1\sin\beta)^2+(z-2mh)^2]^{-\frac{1}{2}} d\xi_1$$

where the first integral term represents the original body plus its reflections in the vertical plane, and the second integral term represents the horizontal image plus its reflections in the vertical plane.

The normal velocity component on the original source distribution located at $x=x_1\cos\beta$, $y=x_1\sin\beta$, and $z=0$ may then be determined. Using this velocity expression and Lagally's theorem, the side force for the body at a given angle β is

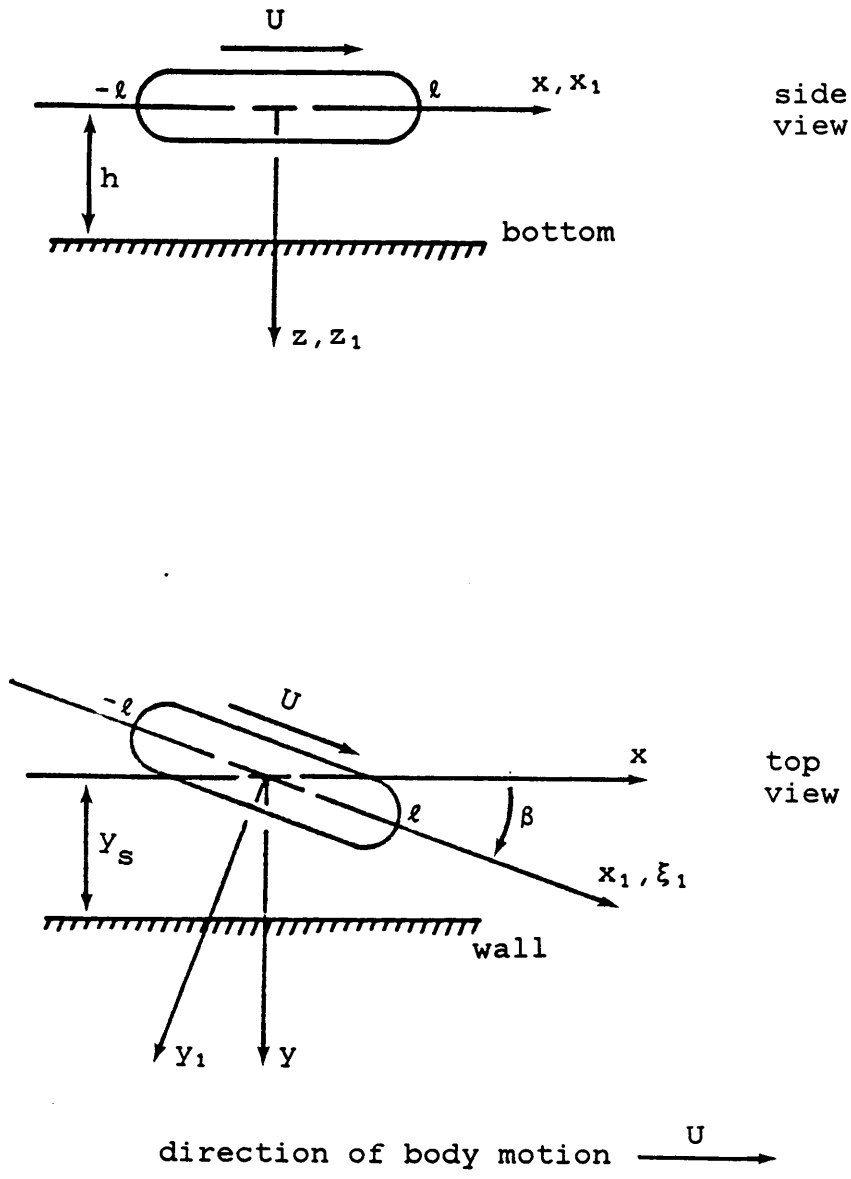

Figure 3. Coordinate System for a Body at an Angle to a Single Wall.

$$Y = \frac{-\rho U^2}{4\pi} \sum_{m=-\infty}^{\infty} \int_{-\ell}^{\ell} S'(x_1) \int_{-\ell}^{\ell} S'(\xi_1) A_1 A \cos\beta \, d\xi_1 \, dx_1 \qquad (13)$$

$$- \frac{\rho U^2}{4\pi} \sum_{m=-\infty}^{\infty} \int_{-\ell}^{\ell} S'(x_1) \int_{-\ell}^{\ell} S'(\xi_1) A_1 (x_1 - \xi_1) \sin\beta \cos\beta \, d\xi_1 \, dx_1$$

where $A_1 = [(x_1\cos\beta - \xi_1\cos\beta)^2 + A^2 + 4m^2h^2]^{-\frac{3}{2}}$

$A = x_1\sin\beta - 2ny_s + \xi_1\sin\beta$

The resultant yaw moment is

$$N = \frac{-\rho U^2}{4\pi} \sum_{m=-\infty}^{\infty} \int_{-\ell}^{\ell} x_1 S'(x_1) \int_{-\ell}^{\ell} S'(\xi_1) A_1 A \cos\beta \, d\xi_1 \, dx_1 \qquad (14)$$

$$- \frac{\rho U^2}{4\pi} \sum_{m=-\infty}^{\infty} \int_{-\ell}^{\ell} x_1 S'(x_1) \int_{-\ell}^{\ell} S'(\xi_1) A_1 (x_1 - \xi_1) \sin\beta \cos\beta \, d\xi_1 \, dx_1$$

where $A_1 = [(x_1\cos\beta - \xi_1\cos\beta)^2 + A^2 + 4m^2h^2]^{-\frac{3}{2}}$

$A = x_1\sin\beta - 2ny_s + \xi_1\sin\beta$

2.1.3 NONDIMENSIONALIZATION

The side force and yaw moment were nondimensionalized in terms of a diameter to length ratio and by using Norrbin's [13] 'bis' system. The 'bis' system of nondimensionalization is a system based on the main hull contour displacement as the reference volume. This form of nondimensionalization was chosen to allow the results of this study to be directly compared to those shown by Newman [11] in his paper. The side force nondimensionalized in this manner is

$$\frac{Y''L^2}{(u'')^2D^2}$$

where from Norrbin's 'bis' system Y" is the nondimensional force, and u" is the Froude number. With ∇_o being the volume displacement at rest, and g the gravitational force, then

$$\frac{Y''L^2}{(u'')^2D^2} = \frac{L^2\ Y/(\rho g \nabla_o)}{D^2\ U^2/(Lg)} = Y\left(\frac{L^3}{\rho \nabla_o\ D^2U^2}\right)$$

For a spheroid $\nabla_o = \pi LD^2/6$. The nondimensional force for a spheroid then can be expressed by

$$\frac{Y''L^2}{(u'')^2D^2} = Y\left(\frac{6L^2}{\pi\rho D^4U^2}\right)$$

The non-dimensional moment is found in a similar manner

$$\frac{N''L^2}{(u'')^2D^2} = N\left(\frac{L^2}{\rho\nabla_o D^2U^2}\right)$$

and for a spheroid,

$$\frac{N''L^2}{(u'')^2D^2} = N\left(\frac{6L}{\pi\rho D^4U^2}\right)$$

2.2 SIDE FORCE AND YAW MOMENT IN A CANAL

2.2.1 BODY PARALLEL TO CANAL WALLS

The problem of a body in shallow water moving parallel to a canal bank is considered next. The canal is of width w, and the body is at a location of $y=y_o$ off the canal centerline in water of depth h as shown in Figure 4. Source distributions will be located at $y=w-y_o$ and $y= -w-y_o$ to satisfy the zero velocity condition on the canal walls. However, the source distribution at $y=w-y_o$ will create a flow on the wall at $y= -w/2$. This is corrected by a source distribution at $y= -2w+y_o$. Likewise, the source distribution at $y= -w-y_o$ is corrected by locating a source distribution at $y=2w+y_o$. This process continues on resulting in an array of source distributions located at $y=nw+(-1)^n y_o$, where n takes on all integer values between $\pm\infty$. The vertical distribution is handled in the same manner as in section 2.1.1, so again

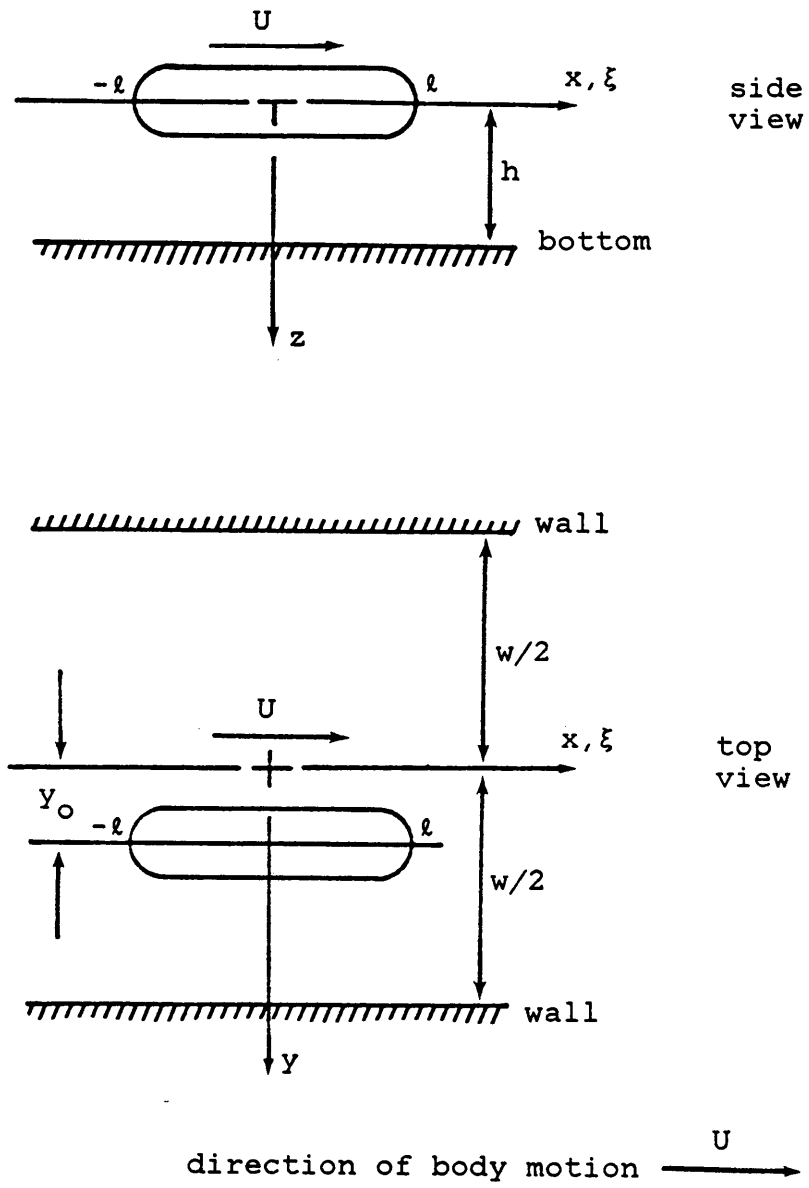

Figure 4. Coordinate System for a Body Parallel to a Canal Wall.

source distributions are located at z=2mh where m takes on all integer values between $\pm\infty$.

The velocity potential in equation (8) may then be written for this case as

$$\phi(x,y,z) = \frac{-U}{4\pi} \sum_{m=-\infty}^{\infty} \sum_{n=-\infty}^{\infty} \int_{-\ell}^{\ell} \{S'(\xi) \times [(x-\xi)^2+(y+nw-(-1)^n y_o)^2+(z-2mh)^2]^{-\frac{1}{2}}\} d\xi$$

This expression includes the original body plus both its horizontal and vertical images.

Lagally's theorem will be used again to determine the side force. The y velocity component evaluated at the location of the original source distribution where x=x, $y=y_o$, and z=0, is expressed in the form of

$$\frac{\partial \phi}{\partial y} = \frac{U}{4\pi} \sum_{m=-\infty}^{\infty} \sum_{\substack{n=-\infty \\ \text{even}}}^{\infty} \int_{-\ell}^{\ell} nwS'(\xi)[(x-\xi)^2+(nw)^2+4m^2h^2]^{-\frac{3}{2}} d\xi$$

$$+ \frac{U}{4\pi} \sum_{m=-\infty}^{\infty} \sum_{\substack{n=-\infty \\ \text{odd}}}^{\infty} \int_{-\ell}^{\ell} \{S'(\xi)(2y_o+nw) \times [(x-\xi)^2+(2y_o+nw)^2+4m^2h^2]^{-\frac{3}{2}}\} d\xi$$

It is evident that the first integral term is zero when n=0. Further examination reveals that for every value cal-

culated for n negative there will be a corresponding value with the opposite sign for n positive in that first integral expression, so that these will sum to zero. Thus, the contribution from the first integral (n even) is zero. Then from Lagally's theorem (equation (10)), the side force is

$$Y = \frac{-\rho U^2}{4\pi} \sum_{m=-\infty}^{\infty} \sum_{\substack{n=-\infty \\ \text{odd}}}^{\infty} \int_{-\ell}^{\ell} S'(x) \int_{-\ell}^{\ell} \{S'(\xi)(2y_o+nw) \times [(x-\xi)^2+(2y_o+nw)^2+4m^2h^2]^{-\frac{3}{2}}\} d\xi dx \tag{15}$$

which is in agreement with the result found by Newman [11].

The resultant yaw moment about the z-axis is

$$N = \frac{-\rho U^2}{4\pi} \sum_{m=-\infty}^{\infty} \sum_{\substack{n=-\infty \\ \text{odd}}}^{\infty} \int_{-\ell}^{\ell} xS'(x) \int_{-\ell}^{\ell} \{S'(\xi)(2y_o+nw) \times [(x-\xi)^2+(2y_o+nw)^2+4m^2h^2]^{-\frac{3}{2}}\} d\xi dx \tag{16}$$

2.2.2 BODY AT AN ANGLE IN A CANAL

The last problem to be considered is that of a body in shallow water moving at a given angle to the canal walls. Again the unsteady effect of a body approaching a wall is neglected and the analysis is for an instantaneous snapshot. The rotated coordinate system for the body is the x_1-axis in the forward direction making an angle β with the canal centerline, the z_1-axis is down, and the y_1-axis is to starboard as shown in Figure 5, with the origin at the body center. The canal is of width w, and the body center is at a distance $y=y_o$ from the canal centerline in water of depth h. Following the same process as in section 2.2.1 for the walls, image source distributions will be located at $y=nw+(-1)^n(y_o+\xi_1 \sin\beta)$, where n takes on all integer values between $\pm\infty$. As in the previous cases, a cascade of source distributions will be located at $z=2mh$ where m takes on all integer values between $\pm\infty$.

The velocity potential in equation (8) may then be written in this case as

$$\phi(x,y,z) = \frac{-U}{4\pi} \sum_{m=-\infty}^{\infty} \sum_{n=-\infty}^{\infty} \int_{-\ell}^{\ell} \{S'(\xi_1)$$

$$\times[(x-\xi_1\cos\beta)^2+[y+nw-(-1)^n(y_o+\xi_1\sin\beta)]^2+(z-2mh)^2]^{-\frac{1}{2}}\}d\xi_1$$

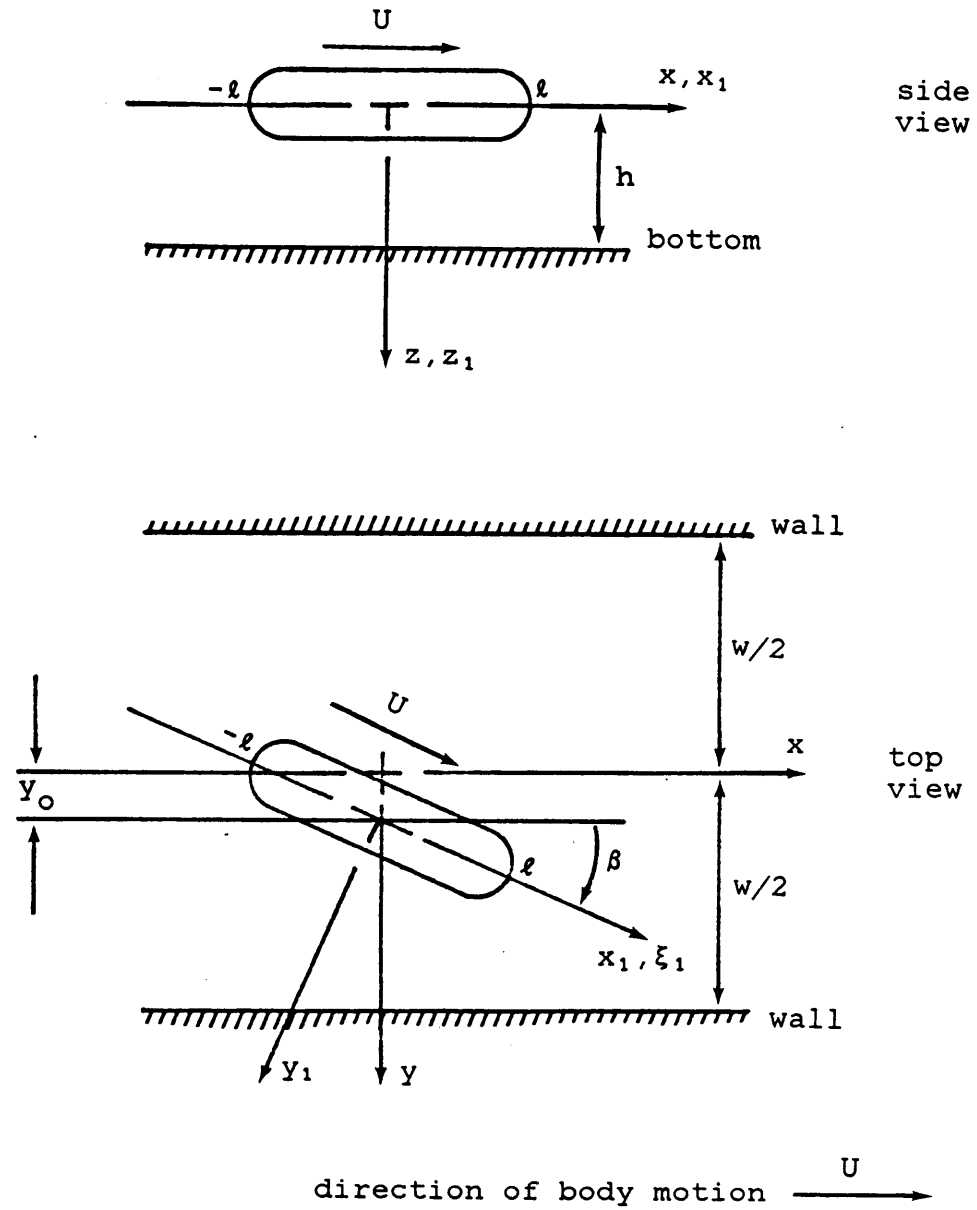

Figure 5. Coordinate System for a Body at an Angle to a Canal Wall.

The resultant normal velocity component at the original source distribution located at $x=x_1\cos\beta$, $y=y_o+x_1\sin\beta$, and $z=0$ may then be found. This velocity expression along with Lagally's theorem gives the side force as

$$Y = \frac{-\rho U^2}{4\pi} \sum_{m=-\infty}^{\infty} \sum_{n=-\infty}^{\infty} \int_{-\ell}^{\ell} S'(x_1) \int_{-\ell}^{\ell} S'(\xi_1) A_1 A \cos\beta \, d\xi_1 dx_1 \qquad (17)$$

$$- \frac{\rho U^2}{4\pi} \sum_{m=-\infty}^{\infty} \sum_{n=-\infty}^{\infty} \int_{-\ell}^{\ell} S'(x_1) \int_{-\ell}^{\ell} S'(\xi_1) A_1 (x_1-\xi_1) \sin\beta\cos\beta \, d\xi_1 dx_1$$

where $A_1 = [(x_1\cos\beta-\xi_1\cos\beta)^2+A^2+4m^2h^2]^{-3/2}$

$A = y_o+x_1\sin\beta+nw-(-1)^n(y_o+\xi_1\sin\beta)$

The resultant yaw moment is

$$N = \frac{-\rho U^2}{4\pi} \sum_{m=-\infty}^{\infty} \sum_{n=-\infty}^{\infty} \int_{-\ell}^{\ell} x_1 S'(x_1) \int_{-\ell}^{\ell} S'(\xi_1) A_1 A \cos\beta \, d\xi_1 dx_1 \qquad (18)$$

$$- \frac{\rho U^2}{4\pi} \sum_{m=-\infty}^{\infty} \sum_{n=-\infty}^{\infty} \int_{-\ell}^{\ell} x_1 S'(x_1) \int_{-\ell}^{\ell} S'(\xi_1) A_1 (x_1-\xi_1) \sin\beta\cos\beta \, d\xi_1 dx_1$$

where $A_1 = [(x_1\cos\beta-\xi_1\cos\beta)^2+A^2+4m^2h^2]^{-3/2}$

$A = y_o+x_1\sin\beta+nw-(-1)^n(y_o+\xi_1\sin\beta)$

2.2.3 NONDIMENSIONALIZATION

The side force and yaw moment in the case of a canal were nondimensionalized in terms of a diameter to length-width ratio and by using Norrbin's [13] 'bis' system. The side force non-dimensionalized in this manner is

$$\frac{Y''wL}{(u'')^2D^2} = Y\left(\frac{wL^2}{\rho\nabla_o D^2U^2}\right)$$

The side force nondimensionalized for a spheroid is

$$\frac{Y''L^2}{(u'')^2D^2} = Y\left(\frac{6wL}{\pi\rho D^4U^2}\right)$$

The non-dimensional moment is

$$\frac{N''wL}{(u'')^2D^2} = N\left(\frac{wL}{\rho\nabla_o D^2U^2}\right)$$

and for a spheroid

$$\frac{N''wL}{(u'')^2D^2} = N\left(\frac{6w}{\pi\rho D^4U^2}\right)$$

3.0 COMPUTATION PROCEDURE

Results were to be determined for two different bodies for angular orientation with respect to either a single wall or a canal bank. The first of these bodies was a spheroid. This is a simple, axisymmetric body shape that allows comparison to the work done by Newman [11]. The second body was a Series 60, block .80 hull that was used to study the application of the slender body theory method presented here to a representative vessel. A longitudinal cross section of each body taken at z=0 is shown in Figure 6. The Series 60, block .80 hull is plotted from an effective diameter, where the effective diameter is calculated from twice the given cross sectional area ($D_e=[8*S(x)/\pi]^{\frac{1}{2}}$).

The evaluation of the spheroid was to be checked at $\beta=0°$ for both the single wall and canal bank cases with results from an exact double integration and numerical summation by the author, and with results presented by Newman [11]. The double integrals in the cases of angular orientation were evaluated by a generalized Gauss-Legendre quadrature [3]. The generalized Gauss-Legendre quadrature for a double integral takes the following form, where the zeros and weight factors can be taken from any reliable table giving zeros and weight factors for Gauss-Legendre quadrature formulas.

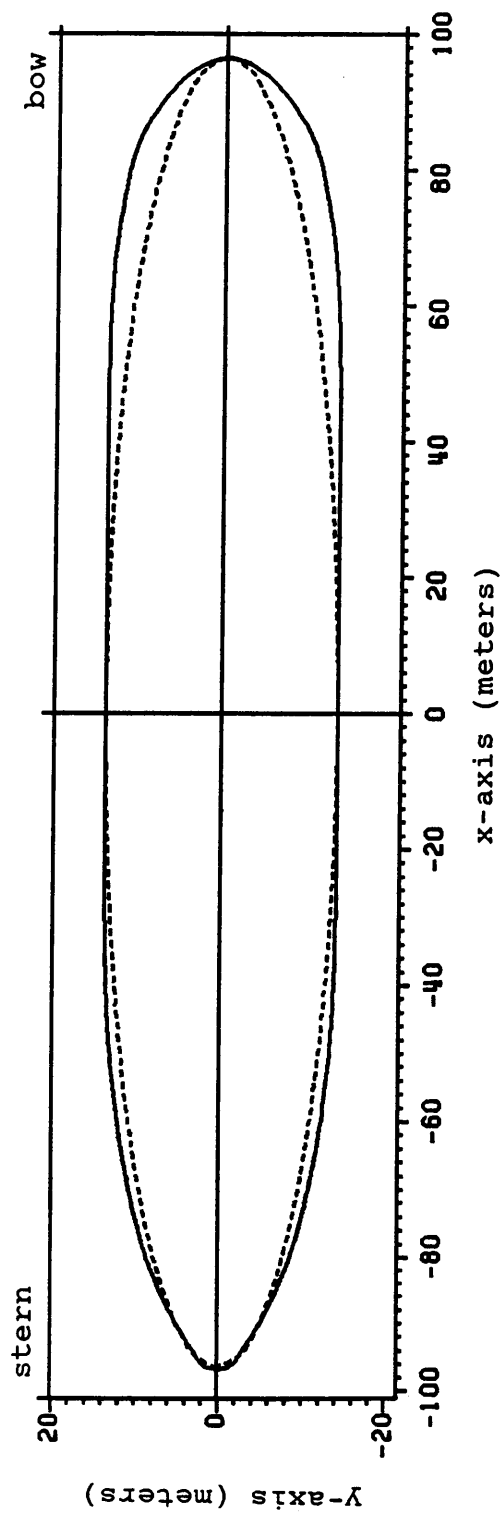

Figure 6. Longitudinal cross section of a spheroid and a Series 60, block .80 hull.

$$\int_a^b \int_c^d f(x,y)dydx \simeq \frac{(b-a)(d-c)}{4} \sum_{j=1}^{M} \sum_{i=1}^{M} W_i W_j f(X,Y)$$

where $X = \frac{1}{2}[x_i(b-a)+b+a]$,

$Y = \frac{1}{2}[y_j(d-c)+d+c]$,

M is the number of point quadrature,

W_i and W_j are the weight factors,

and x_i and y_j are the zeros.

Representative computer programs are located in Appendices A and B. Appendix A presents the program for the nondimensional side force on a spheroid in near proximity to a single wall in shallow water. This program is easily adapted to the yaw moment, see equations (15) and (16), by changing the multiplying constant and inserting the extra term in the outer integral. The Series 60, block .80 hull side force and yaw moment programs are identical to those of the spheroid, except for the insertion of the ship's cross sectional areas and dimensions. It should be noted that the values for the cross sectional areas entered into the program are twice those given for the ship due to the double body approach taken in the development of the problem. Appendix B lists the program for the yaw moment on a Series 60, block .80 hull in a canal in shallow water. This program can also easily be adapted to the other cases, with similar changes as described above.

4.0 RESULTS AND DISCUSSION

Results are presented for a spheroid and a Series 60, block .80 hull moving in shallow water in proximity to either a single wall or canal bank. For each body, results for angular orientation up to 25° are presented, along with variations in separation distance and water depth.

4.1 SIDE FORCE AND YAW MOMENT FOR A SINGLE WALL

Results for a spheroid running parallel to a single wall are shown in Figure 7, along with points taken from Newman's [11] results by a Tektronix 4956 Digitizer. Figure 7 shows excellent agreement between the results found here and the results presented by Newman. It is seen that the bank suction force increases as separation distance from the wall is decreased. The reduction of water depth also has the effect of increasing the side force. It should be noted that a depth of h/L=1.0 is effectively an infinite depth. These results are in agreement with both theoretical and experimental results found by others [2,4,6,7]. Results for the Series 60, block .80 hull running parallel to a single wall are shown in Figure 8. These results follow the same trends as those for the spheroid.

In Figure 9, the results at $\beta=10°$ are shown for the spheroid. Here it can be seen that the same general trends of increased bank suction force with reduction of separation distance and decreasing water depth occur. Due to the symmetry of the spheroid, the method presented here predicts an angle of $\beta=-10°$ to produce the same results as those for $\beta=10°$. In Figure 10 and Figure 11, it can be seen how the magnitude of the resultant force predicted by this method is dependent on the sign of the angle due to the asymmetry of the Series 60, block .80 hull. However, it would be expected that the spheroid would experience different forces approaching or moving away from the wall, and is predicted to have the same force due to neglecting the unsteady effects. The effect of various angles of approach to the wall at a particular depth are shown in Figure 12 and Figure 13. Increasing angle seems to indicate an increase in the bank suction force, although this effect is negligible at distances greater than L/2 away from the wall. These results do not agree with those found by Dand [6] and Hess [7] reproduced in Figure 17 and Figure 18 respectively. They find that an increased angle will decrease the resultant side force. These results are not plotted against results presented by this paper due to the differences in modeling parameters. The qualitative results presented by Dand and Hess are based on observed experimentation. These results are also confirmed by experienced ship pilots [6].

Studying the yaw moment, it is seen for the spheroid in Figure 14 that the resultant moment is bow toward the wall (clockwise) for an angle of $\beta=10°$. As the separation distance increases, it can be seen that the resultant yaw moment is reduced, tending to zero at large separation distances. This is expected because the yaw moment on a body in an unbounded ideal fluid would be zero. An angle of $\beta=-10°$ shows the opposite effects as those for $\beta=10°$, but of the same magnitude for the spheroid. The Series 60, block .80 hull follows the same trends as the spheroid, except for different magnitudes at $\pm\beta$ due to the asymmetry of the hull. The effect of increasing angle at a given depth are presented in Figure 15 and Figure 16. Here increased angle is observed to increase the yaw moment, again in contradiction to the results by Dand [6] and Hess [7] shown in Figure 17 and Figure 18 respectively. They predict an increase in angle will decrease the resultant yaw moment. It can also be seen by comparing Figure 15 and Figure 16, that at $\beta=0°$ the spheroid has a zero moment, whereas the Series 60 block .80 hull is predicted to have a bow to wall moment at the same orientation. This shows that although the method used here correctly predicts a zero moment on a fore and aft symmetric body parallel to a wall, the method is unable to correctly predict the variations associated with realistic ship forms.

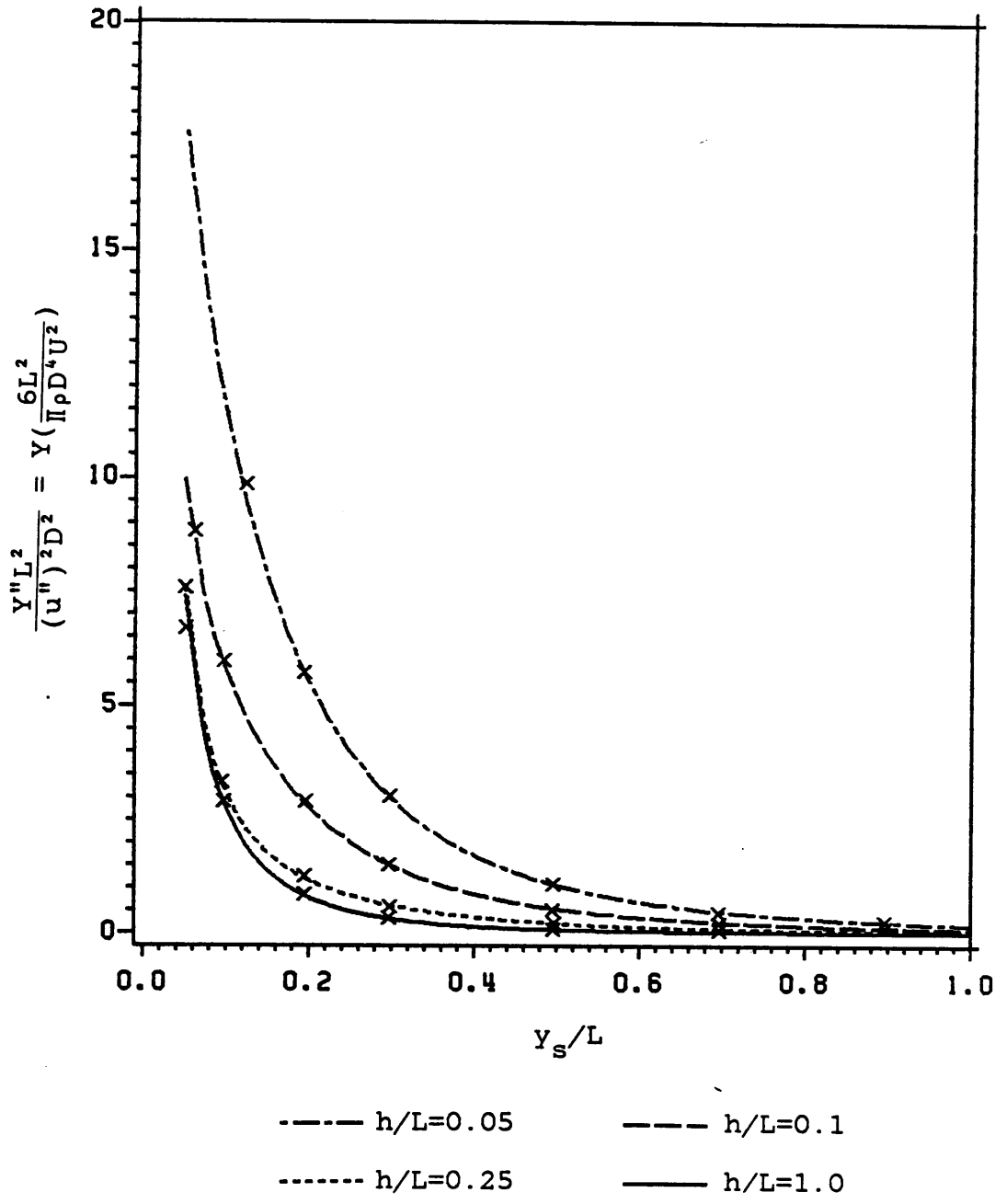

Figure 7. Variation of Bank Suction Force with Lateral Position at Various Water Depths for a Spheroid at $\beta = 0°$.

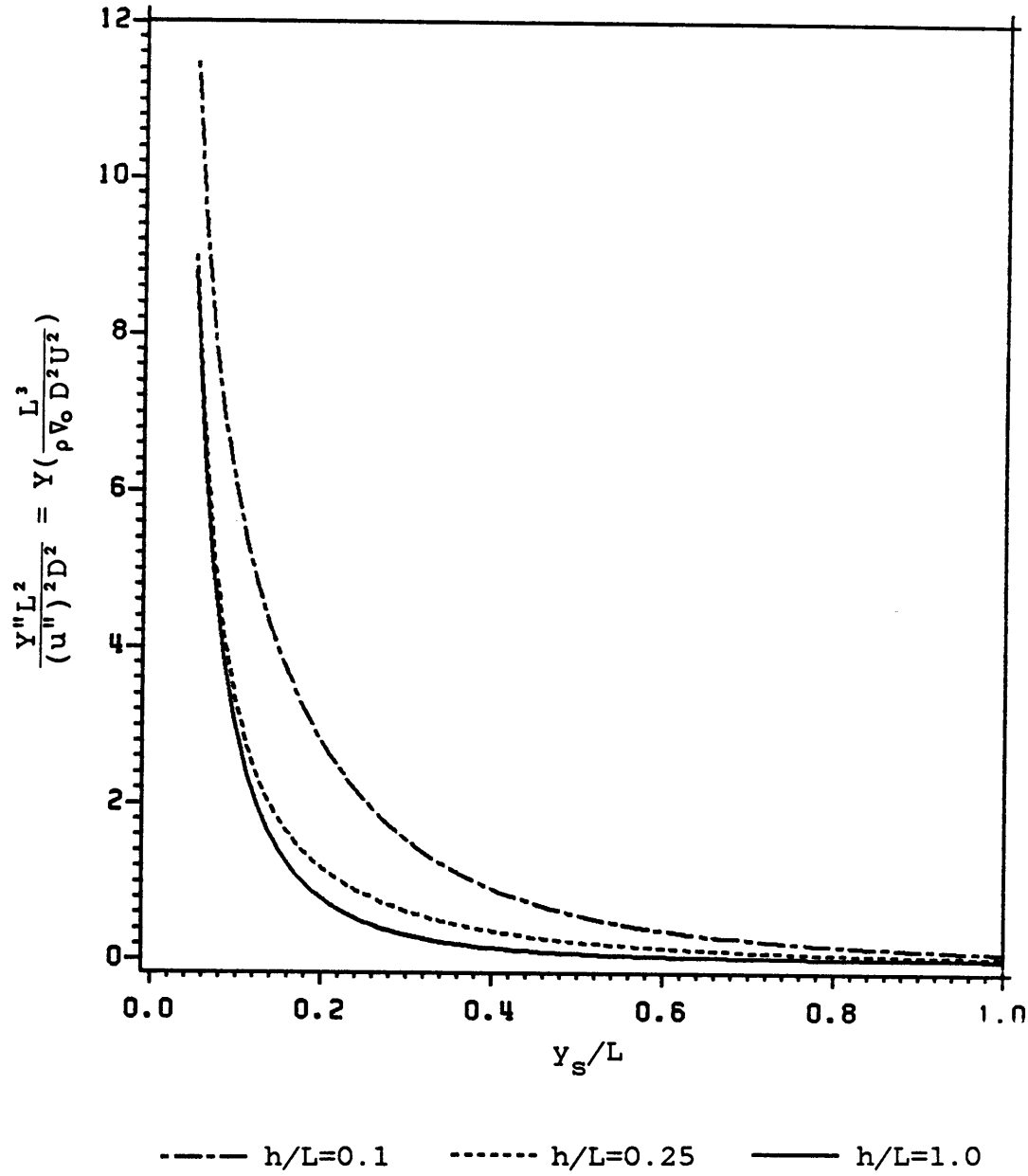

Figure 8. Variation of Bank Suction Force with Lateral Position at Various Water Depths for a Series 60, Block .80 Hull at $\beta = 0°$.

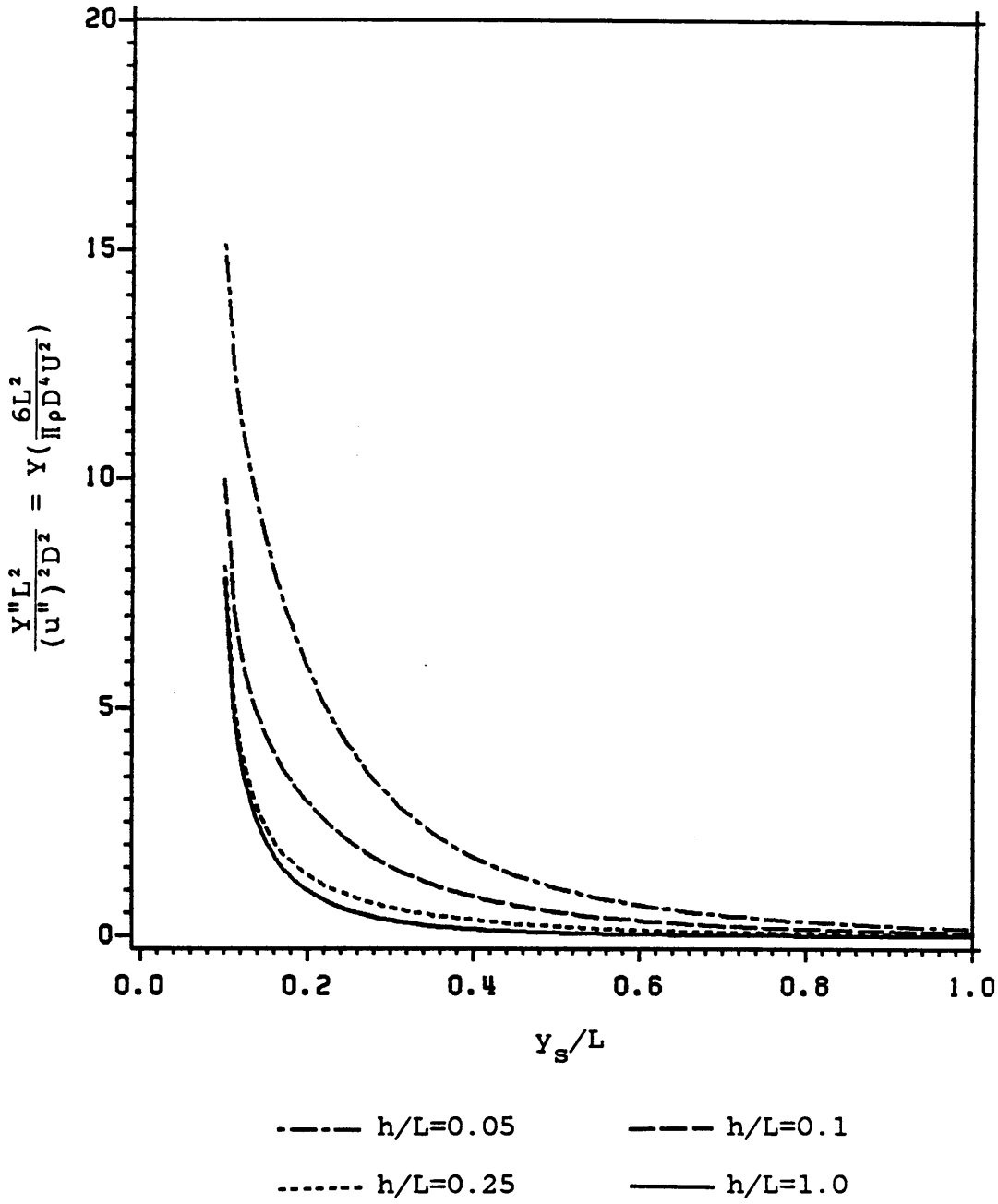

Figure 9. Variation of Bank Suction Force with Lateral Position at Various Water Depths for a Spheroid at $\beta = 10°$.

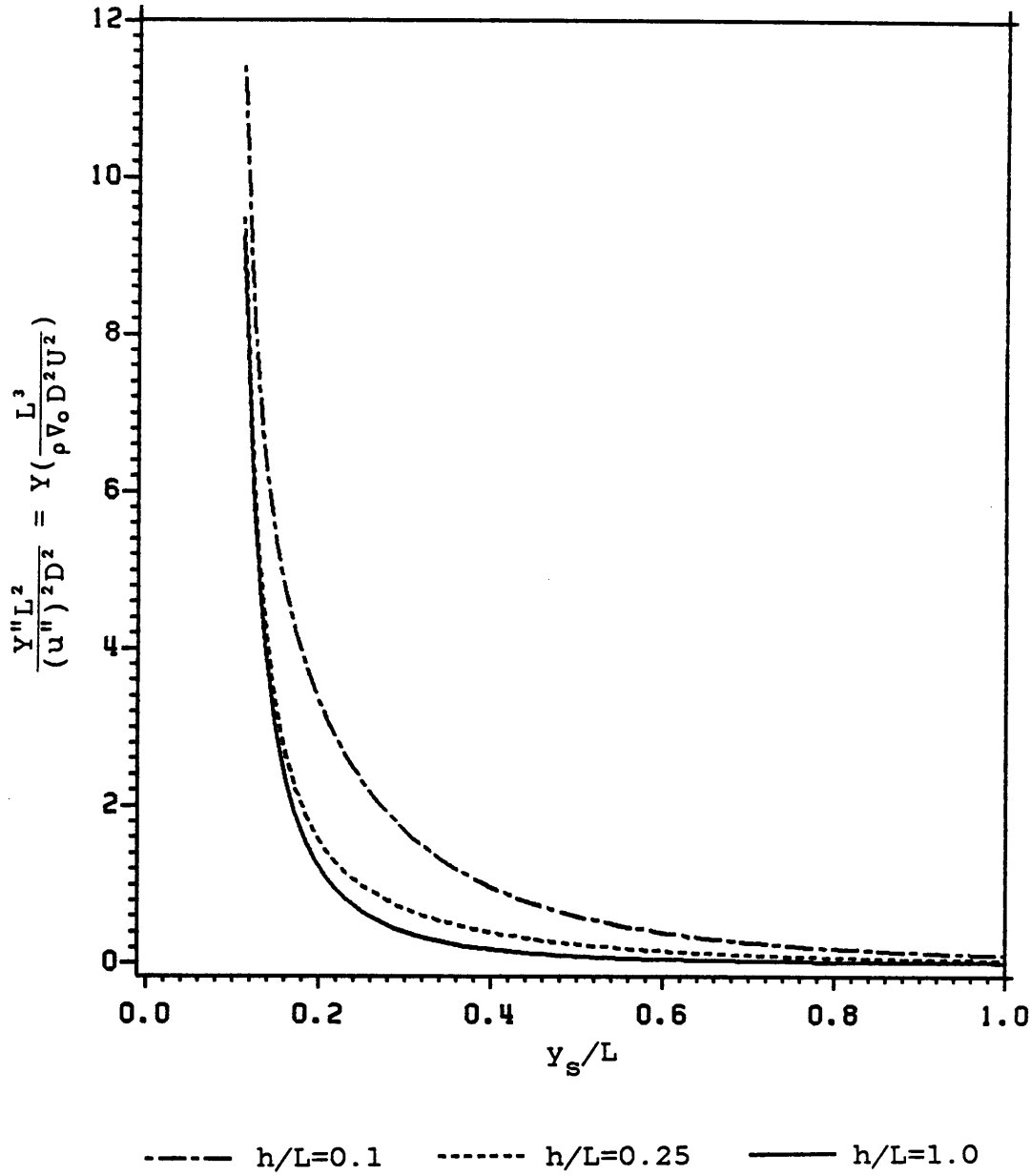

Figure 10. Variation of Bank Suction Force with Lateral Position at Various Water Depths for a Series 60, Block .80 Hull at $\beta = 10°$.

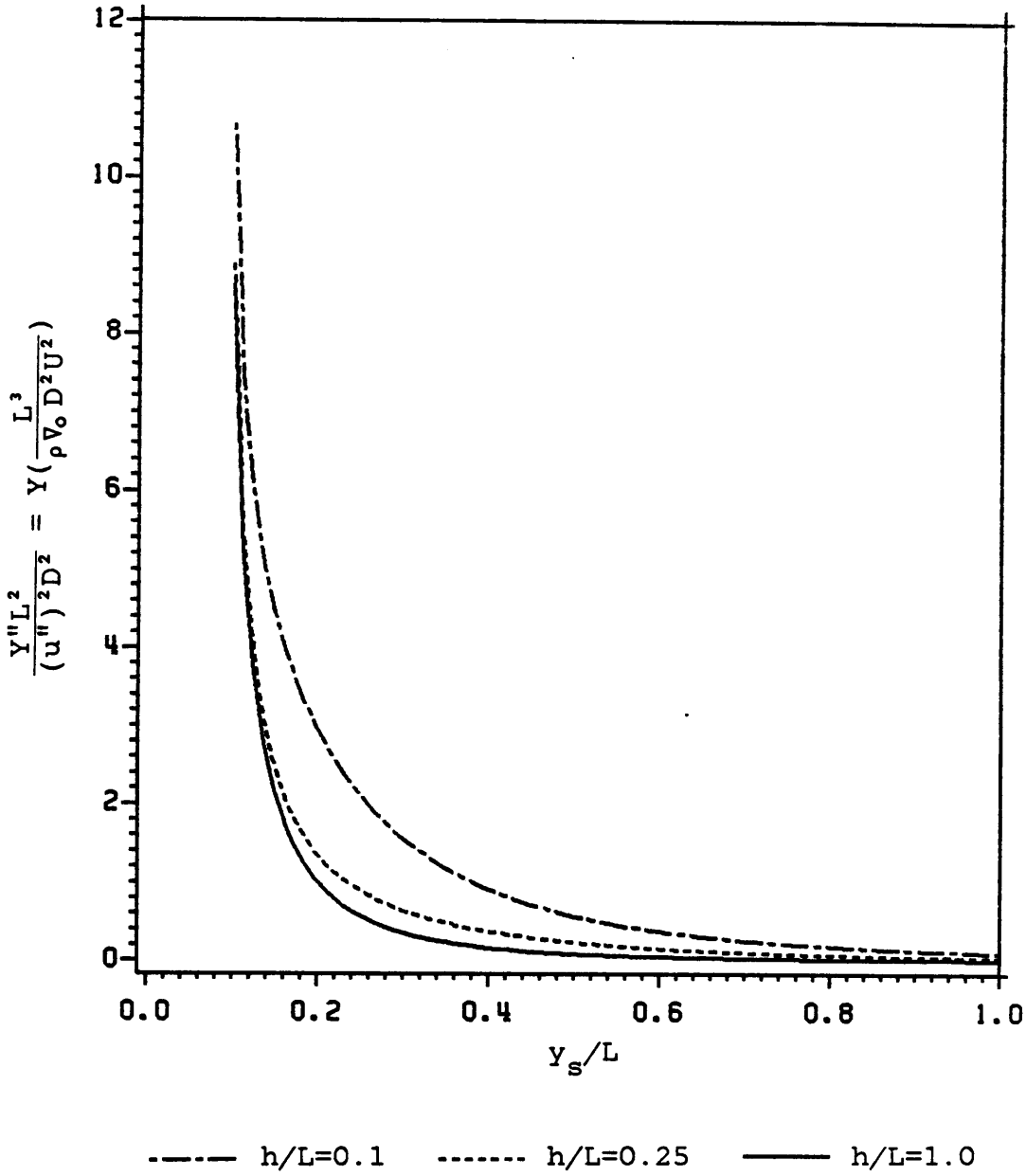

Figure 11. Variation of Bank Suction Force with Lateral Position at Various Water Depths for a Series 60, Block .80 Hull at $\beta = -10°$.

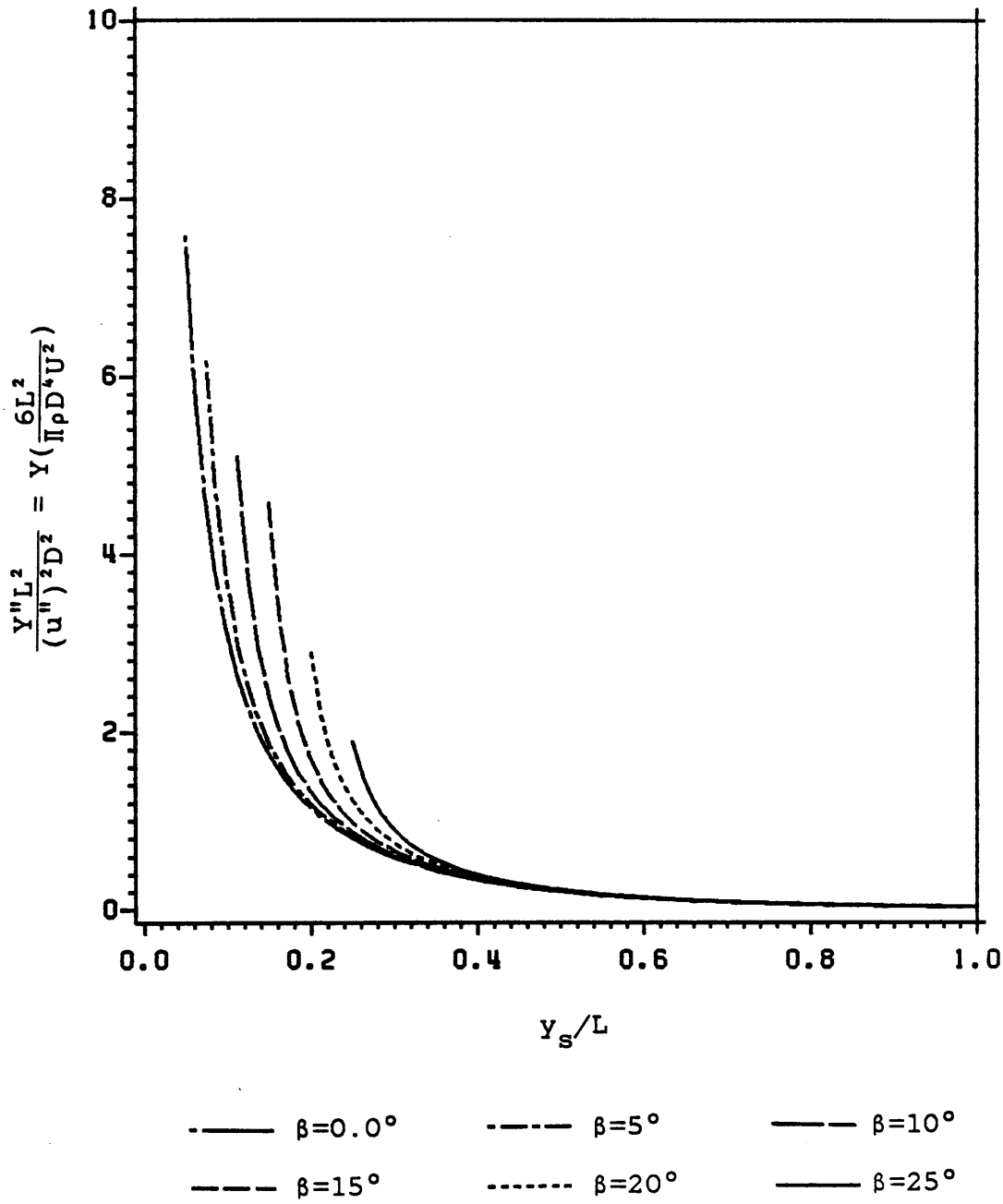

Figure 12. Variation of Bank Suction Force with Lateral Position at Various Angles for a Spheroid at a Fixed Water Depth of h/L=.25.

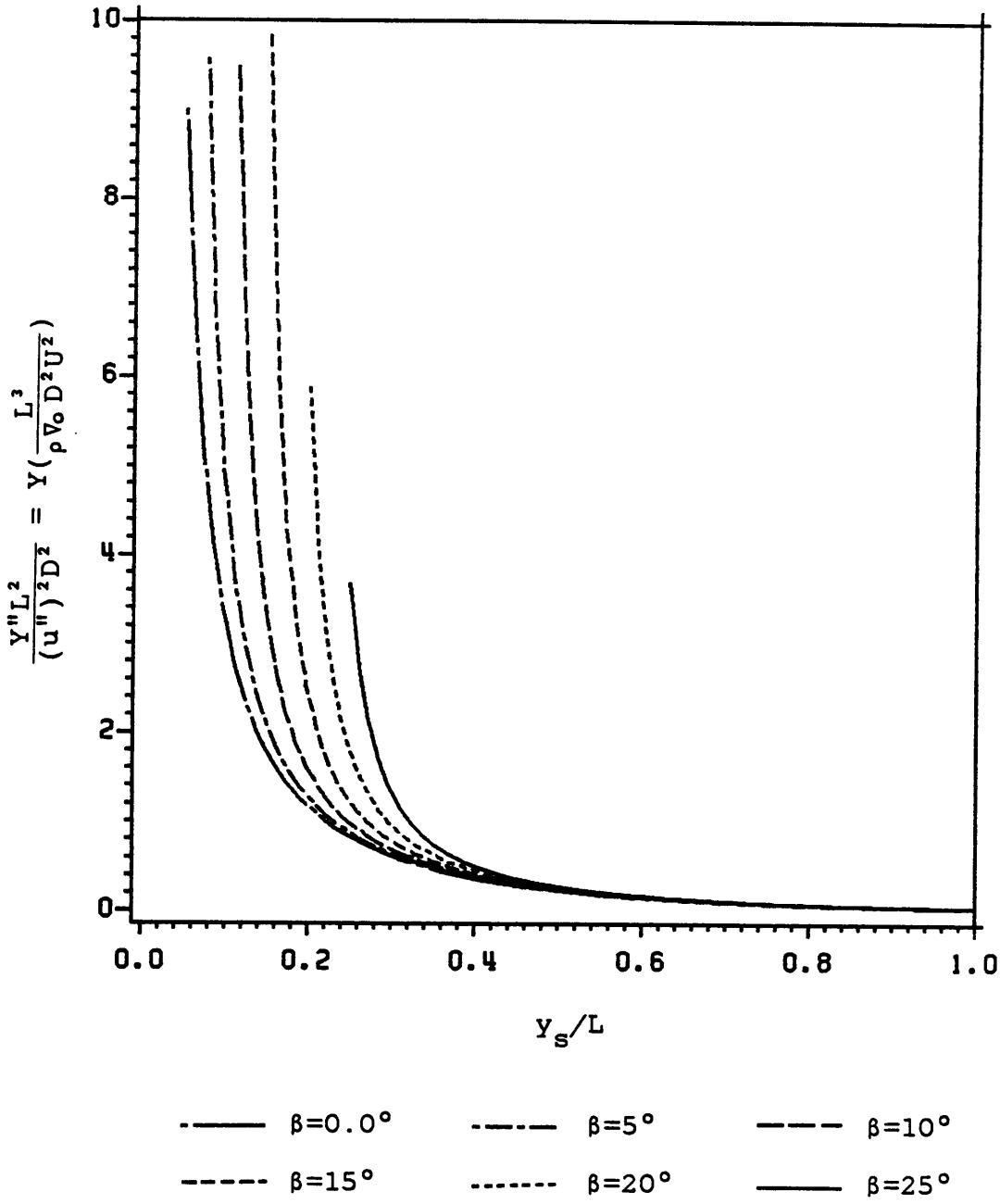

Figure 13. Variation of Side Force with Lateral Position at Various Angles for a Series 60, Block .80 Hull at a Fixed Water Depth of h/L=.25.

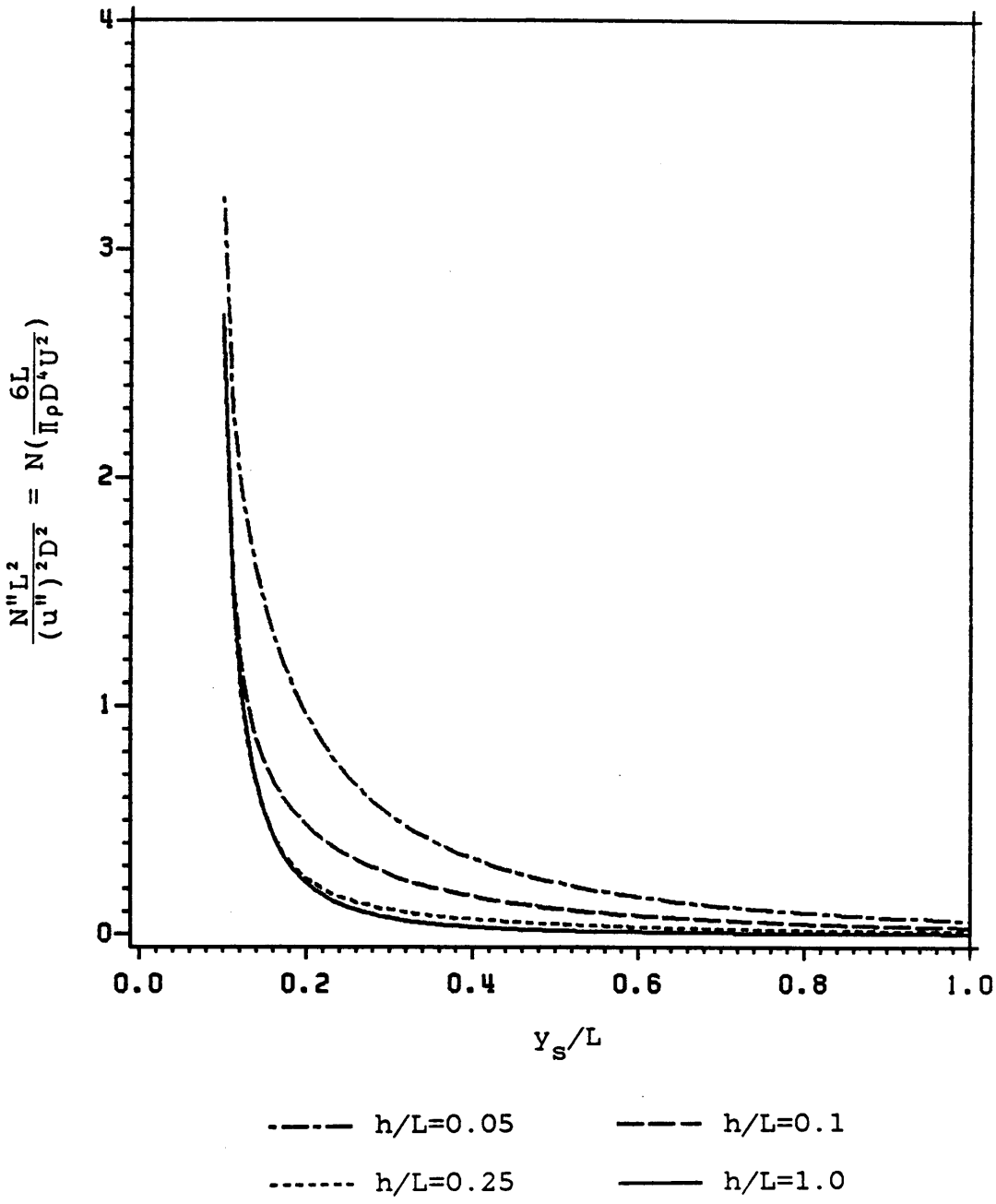

Figure 14. Variation of Yaw Moment with Lateral Position Near a Single Wall at Various Water Depths for a Spheroid at $\beta = 10°$.

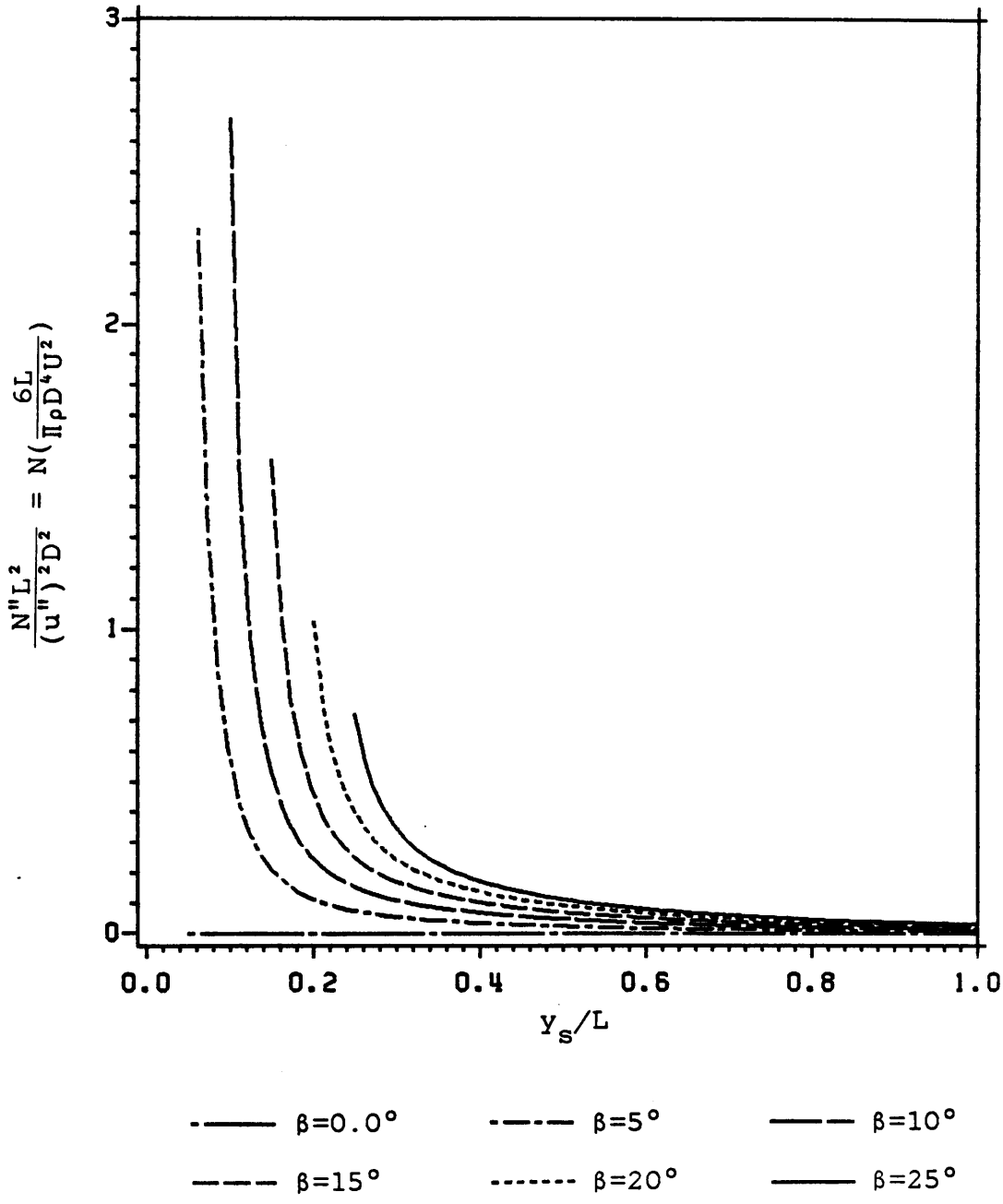

Figure 15. Variation of Yaw Moment with Lateral Position Near a Single Wall at Various Angles for a Spheroid at a Fixed Water Depth of h/L=.25.

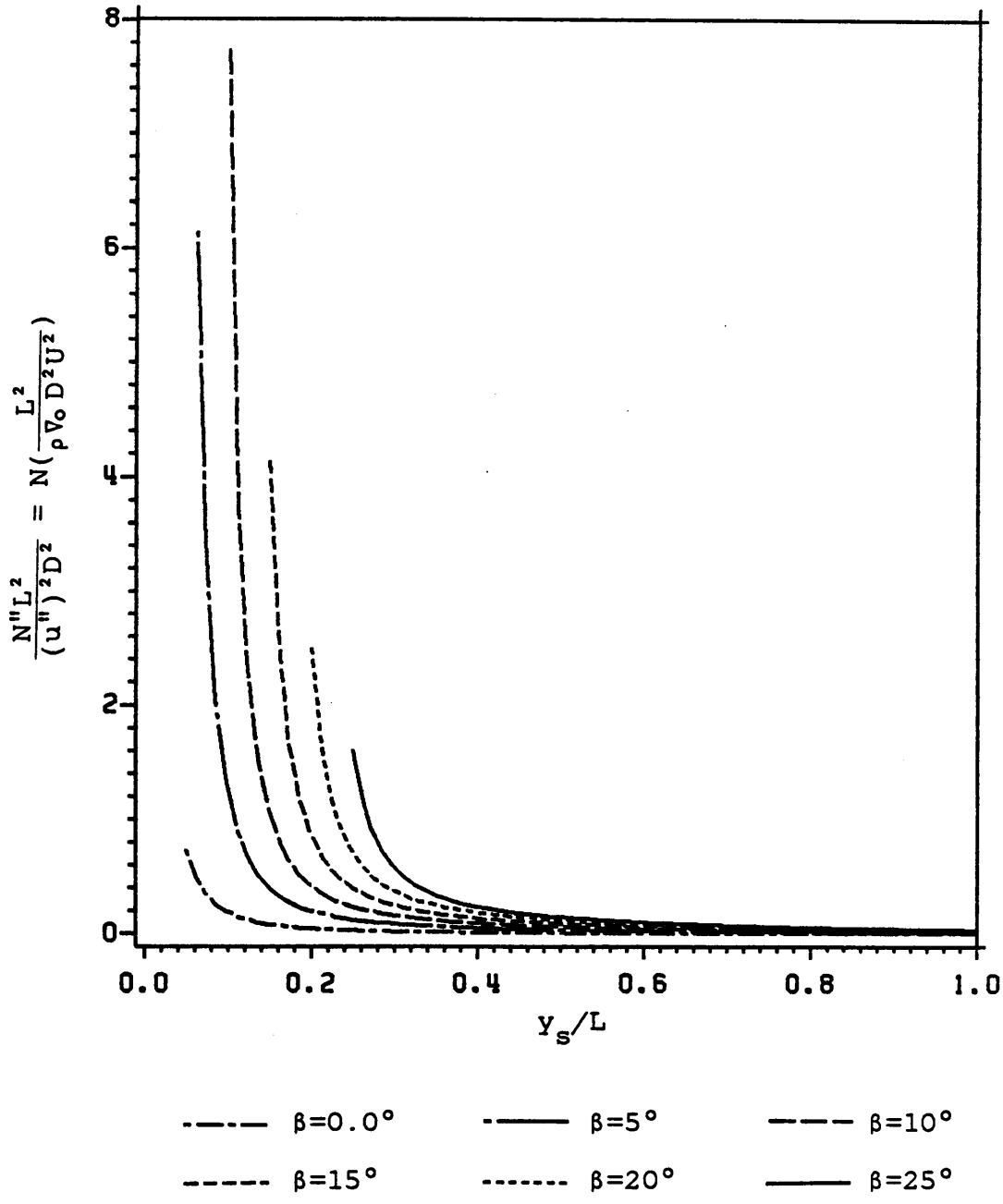

Figure 16. Variation of Yaw Moment with Lateral Position Near a Wall at Various Angles for a Series 60, Block .80 Hull at a Depth of h/L=.25.

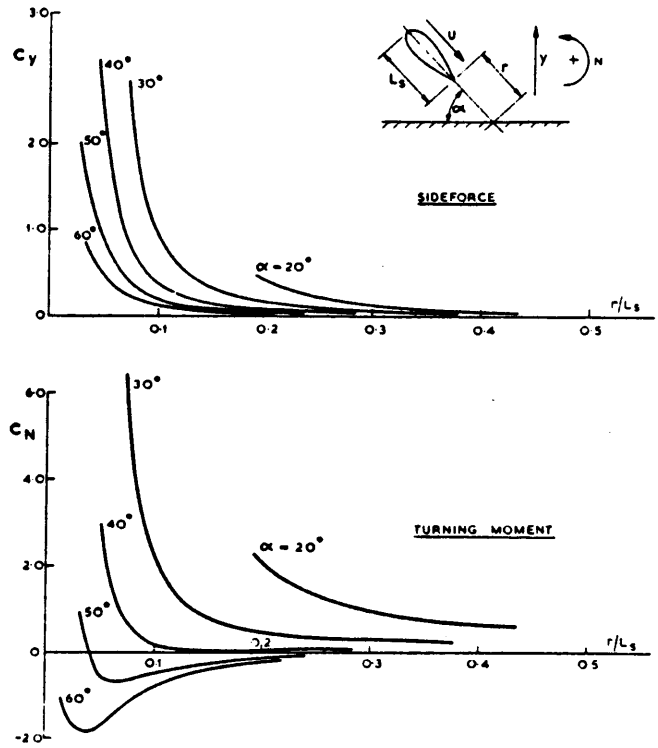

Calculated Bank Rejection Forces and Moments

C_N	turning moment coefficient
C_Y	lateral force coefficient

Figure 17. Side Force and Yaw Moment Results from Dand [6].

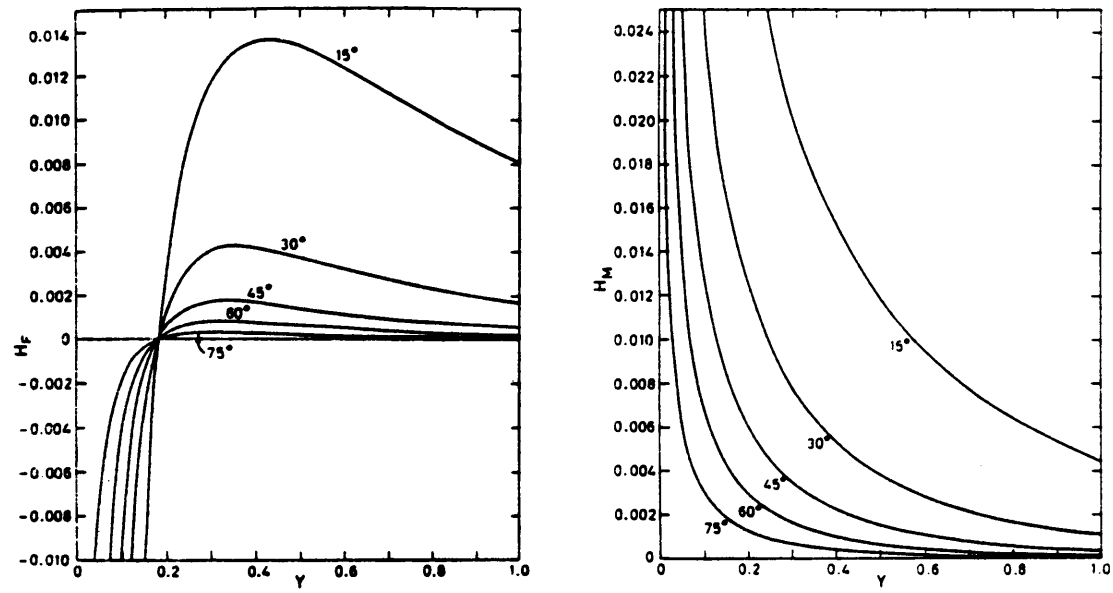

$W = 1$; $c/d = 0.1$; numbers with curves denote values for $\frac{1}{2}\Psi$.

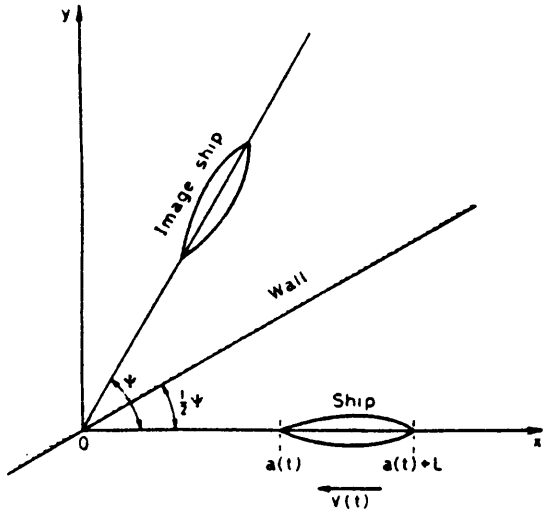

Coordinate system and geometry of the problem

c/d = clearance-to-draft ratio

$H_F(Y)$ = dimensionless sway force

$H_M(Y)$ = dimensionless yaw moment

$W(Y)$ = ship's dimensionless velocity

Y = distance from bow to impact point in ship lengths

Ψ = twice angle between ship's course and wall

Figure 18. Side Force and Yaw Moment Results from Hess [7].

4.2 SIDE FORCE AND YAW MOMENT IN A CANAL

The results for a spheroid moving parallel to a canal wall are found to be identical to those presented by Newman [11] and are shown in Figure 19. The side force increases as the spheroid moves away from the canal centerline towards the wall. Reduction of depth also increases the side force. It should be observed that the far wall tends to cancel the effects of the near wall until close proximity to the near wall. This effect has also been observed by Beck [2] and Cohen and Beck [4]. The results of the Series 60, block .80 hull running parallel to a canal wall are seen to have the same general trends as those of the spheroid, as shown in Figure 20.

For a spheroid at an angle of $\beta=10°$, as shown in Figure 21, there is a marked dependence upon the canal width, as can also be seen in the previous two figures. The same general trends of increasing force with increased distance from the canal centerline and reduction of water depth are also observable. The effect of the sign of the angle shows up only for the Series 60, block .80 hull. This can be seen in Figure 22 and Figure 23. Again the narrower canal shows a marked effect upon the results. The asymmetry of the body is also evident at the canal centerline. The effect of angle at a constant depth can be observed in Figure 24 and Figure 25. These figures show an increase in side force with

an increase in angular orientation. As in the case of a single wall, this result does not agree with that observed by Dand [6] as seen in Figure 17. Dand observed that an increase in angle decreased the side force.

In Figure 26 it is seen for a spheroid that a bow to wall moment is produced at the canal centerline when the spheroid is oriented at $\beta=10°$. Again, a reduced depth increases the moment. Evaluation at $\beta=-10°$ shows the same trends, except it is a bow away from wall moment that is predicted. The Series 60, block .80 hull follows the same patterns, except the moments are of different magnitudes at plus and minus angles due to the asymmetry of the hull. Increased angle is observed to cause an increase in the moment in Figure 27 and Figure 28, contrary to the results found by Dand [6] shown in Figure 17. As in the case of a single wall, the results for a spheroid at $\beta=0°$ are correct, but the method again is unable to correctly predict results for a realistic ship form.

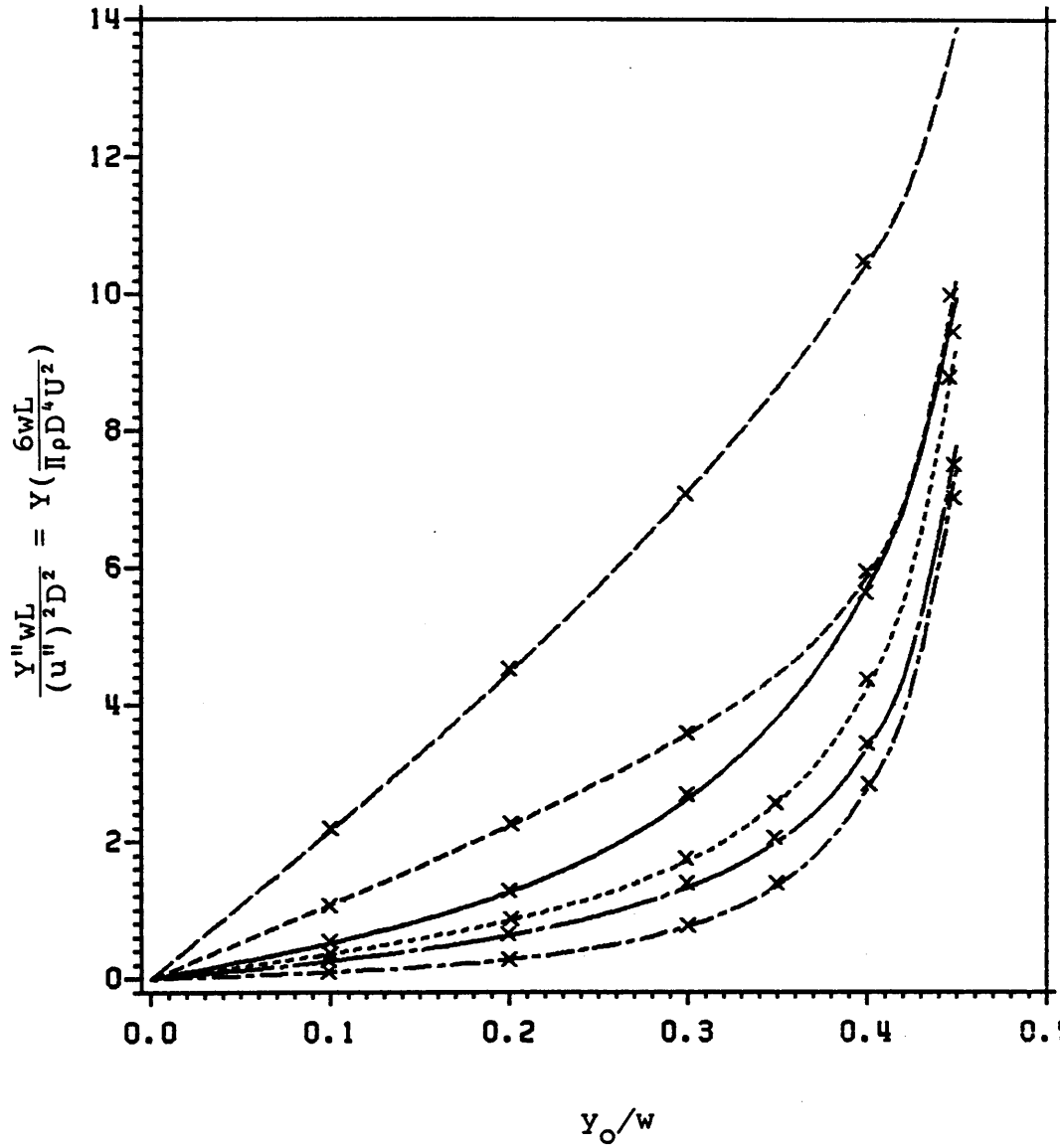

Figure 19. Variation of Side Force with Lateral Position at Various Canal Widths and Depths for a Spheroid at $\beta = 0°$.

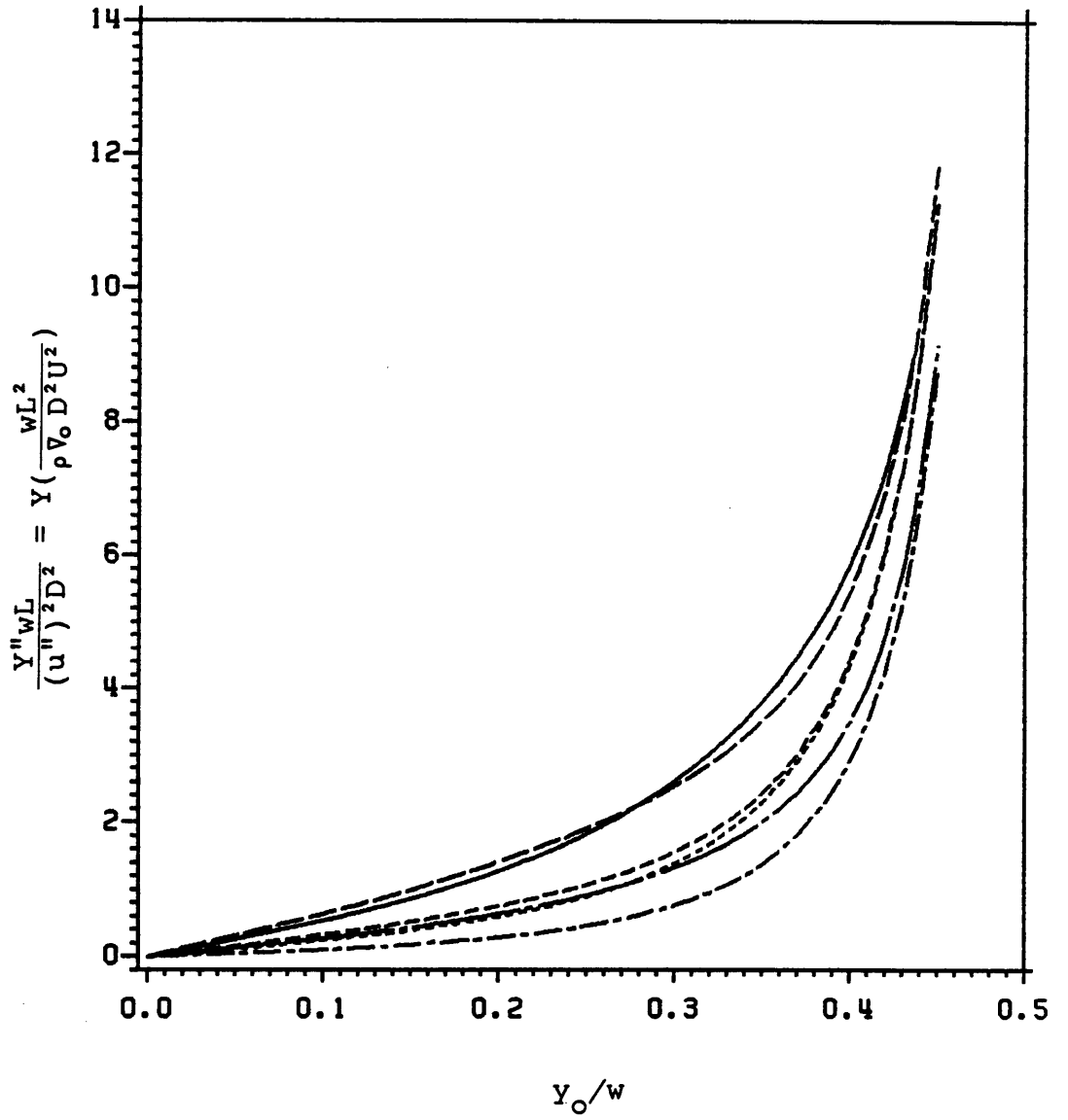

Figure 20. Variation of Side Force with Lateral Position at Various Canal Widths and Depths for a Series 60, Block .80 Hull at $\beta = 0°$.

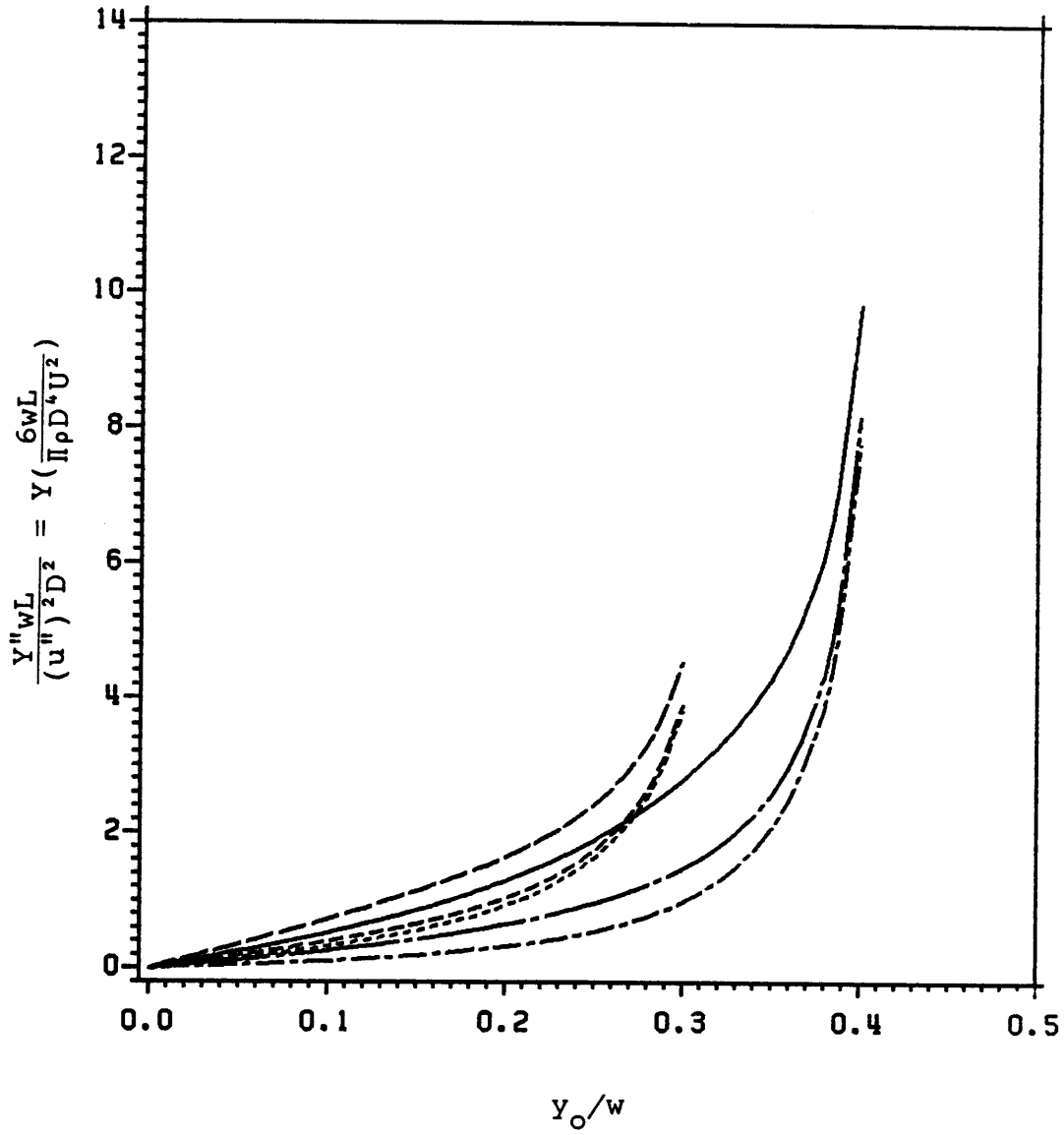

Figure 21. Variation of Side Force with Lateral Position at Various Canal Widths and Depths for a Spheroid at $\beta = 10°$.

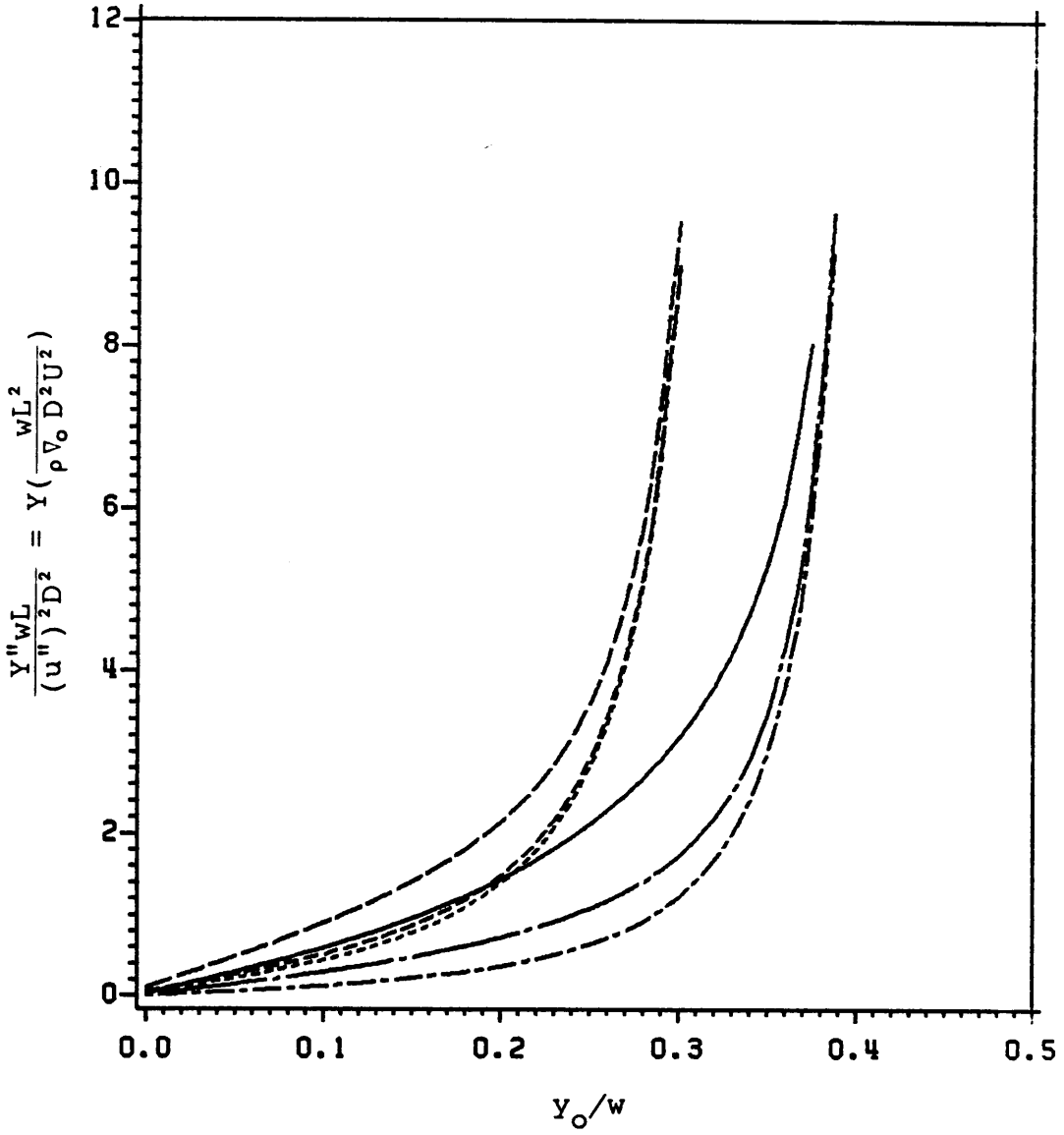

Figure 22. Variation of Side Force with Lateral Position at Various Canal Widths and Depths for a Series 60, Block .80 Hull at $\beta = 10°$.

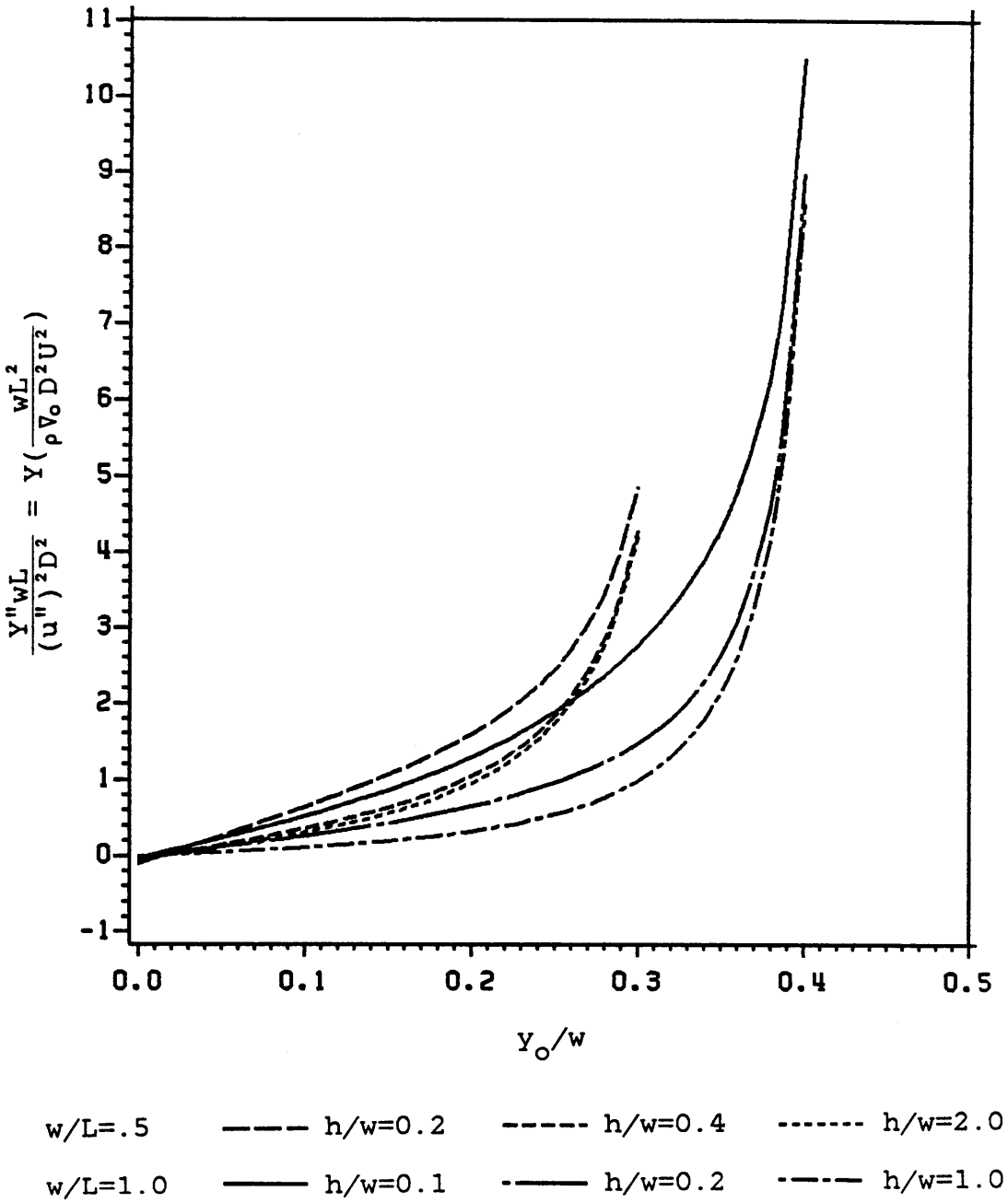

Figure 23. Variation of Side Force with Lateral Position at Various Canal Widths and Depths for a Series 60, Block .80 Hull at β = -10°.

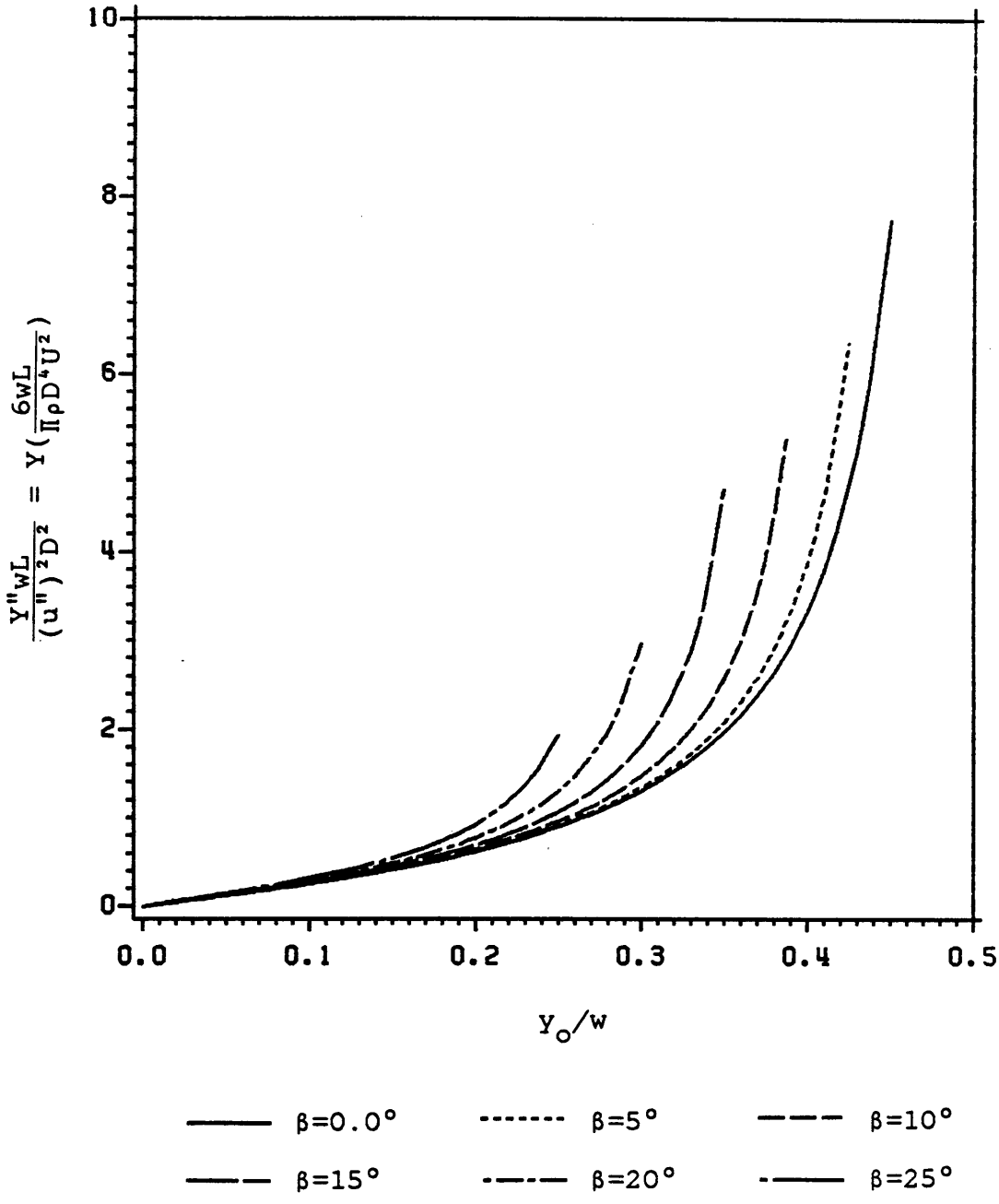

Figure 24. Variation of Side Force with Lateral Position at Various Angles for a Spheroid at a Fixed Canal Width and Depth of w/L=1 and h/w=.2.

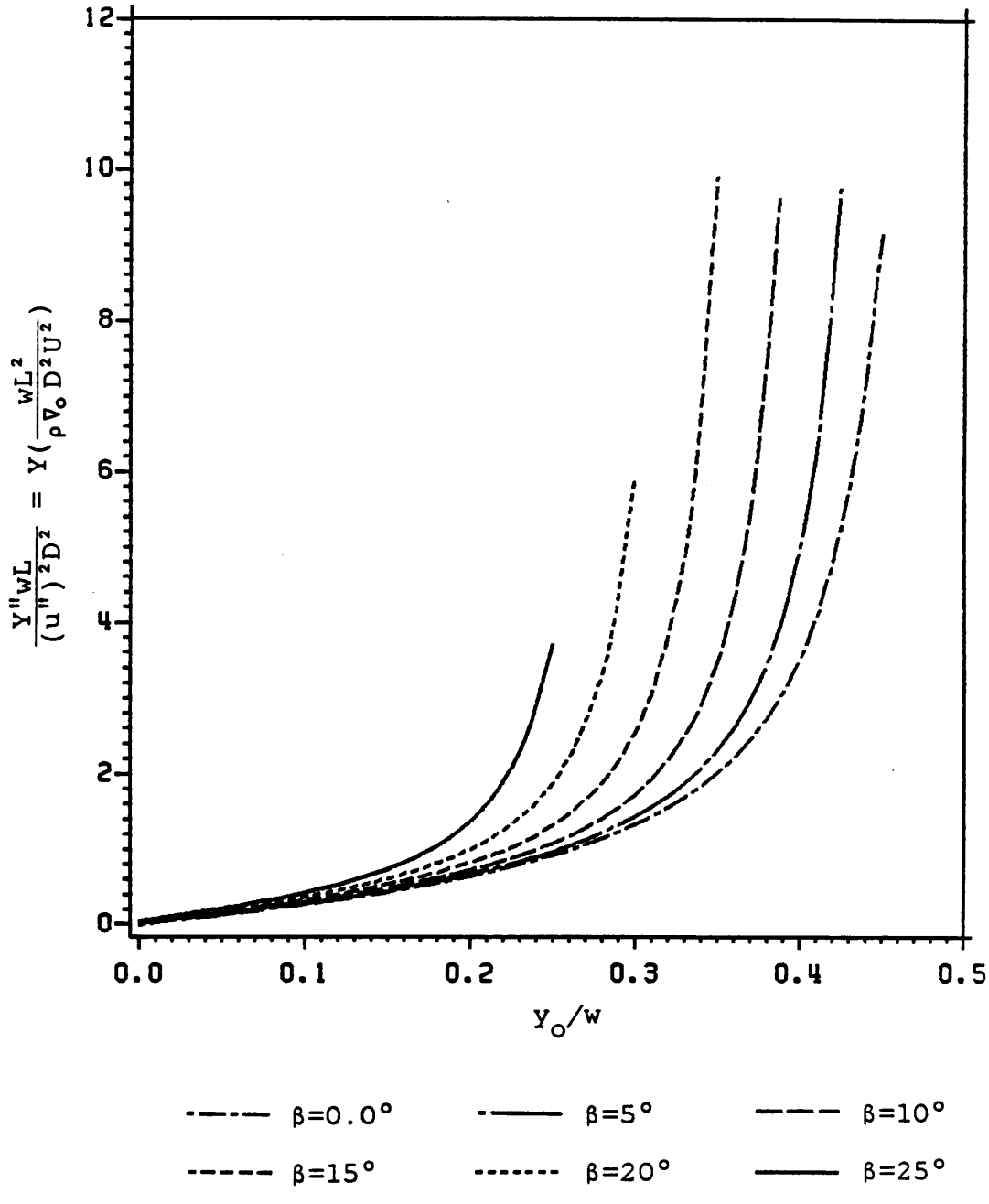

Figure 25. Variation of Force with Lateral Position at Various Angles for a Series 60, Block .80 Hull at a Width and Depth of w/L=1 and h/w=.2.

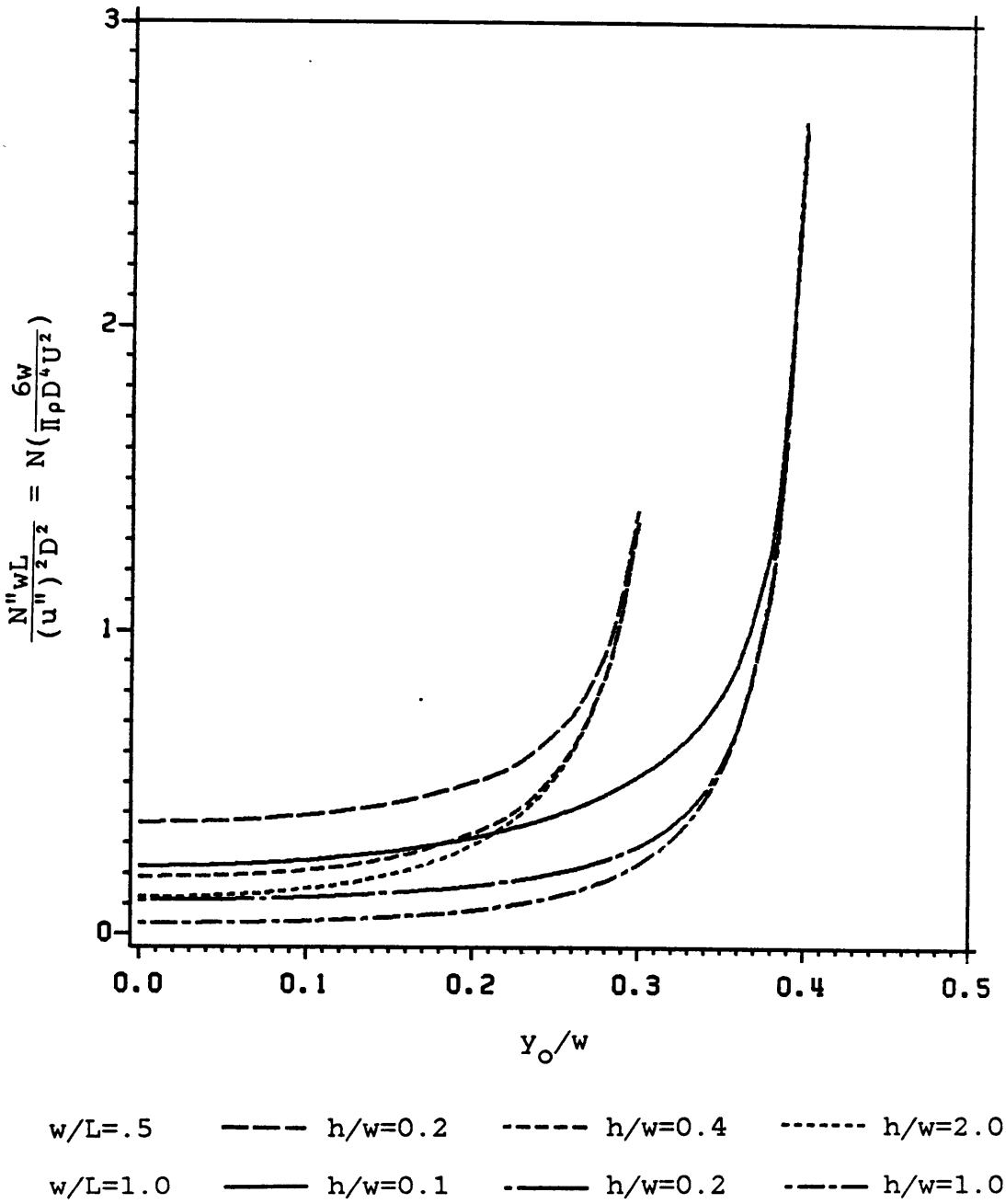

Figure 26. Variation of Yaw Moment with Lateral Position at Various Canal Widths and Depths for a Spheroid at $\beta = 10°$.

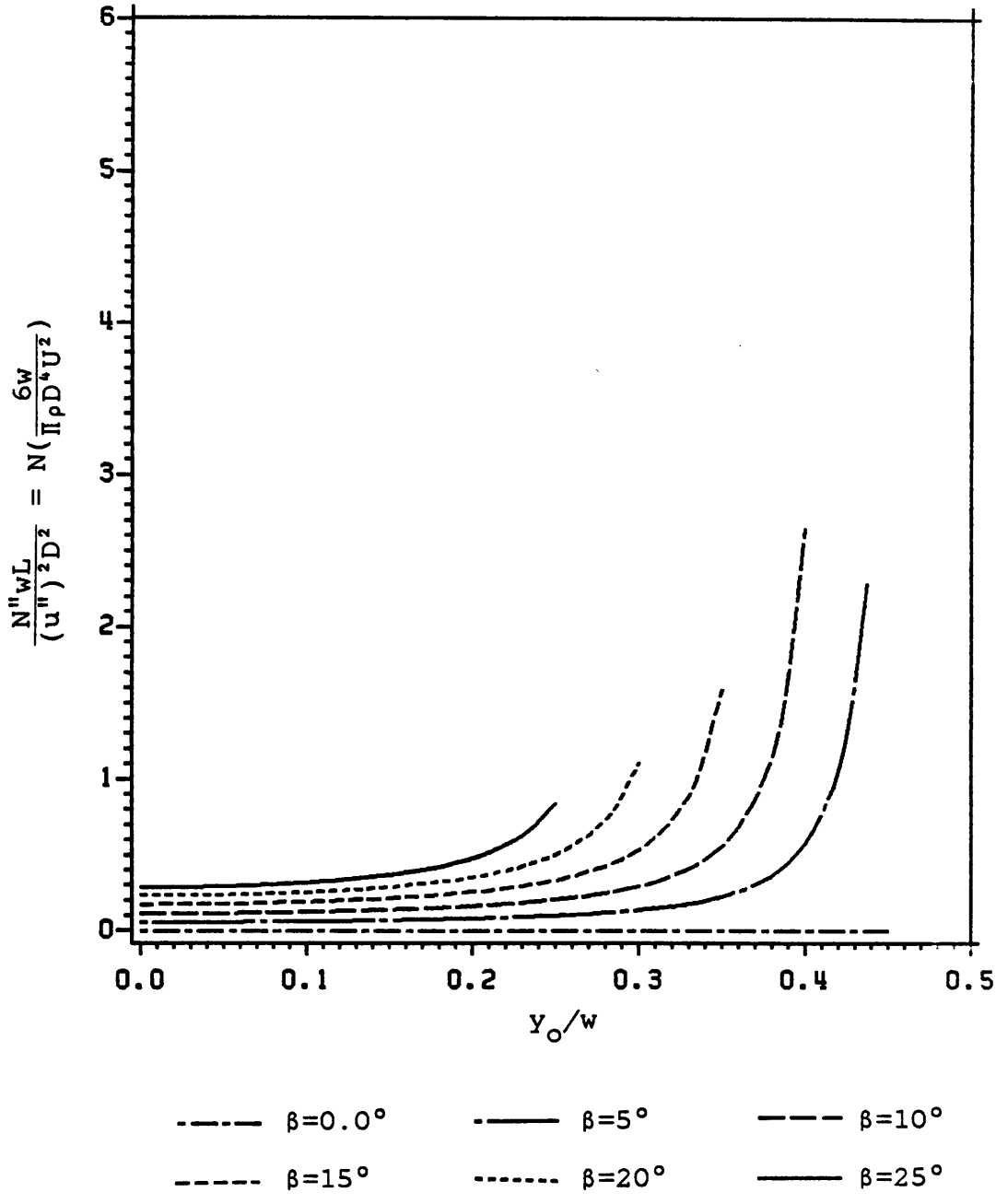

Figure 27. Variation of Yaw Moment with Lateral Position at Various Angles for a Spheroid at a Fixed Canal Width and Depth of w/L=1 and h/w=.2.

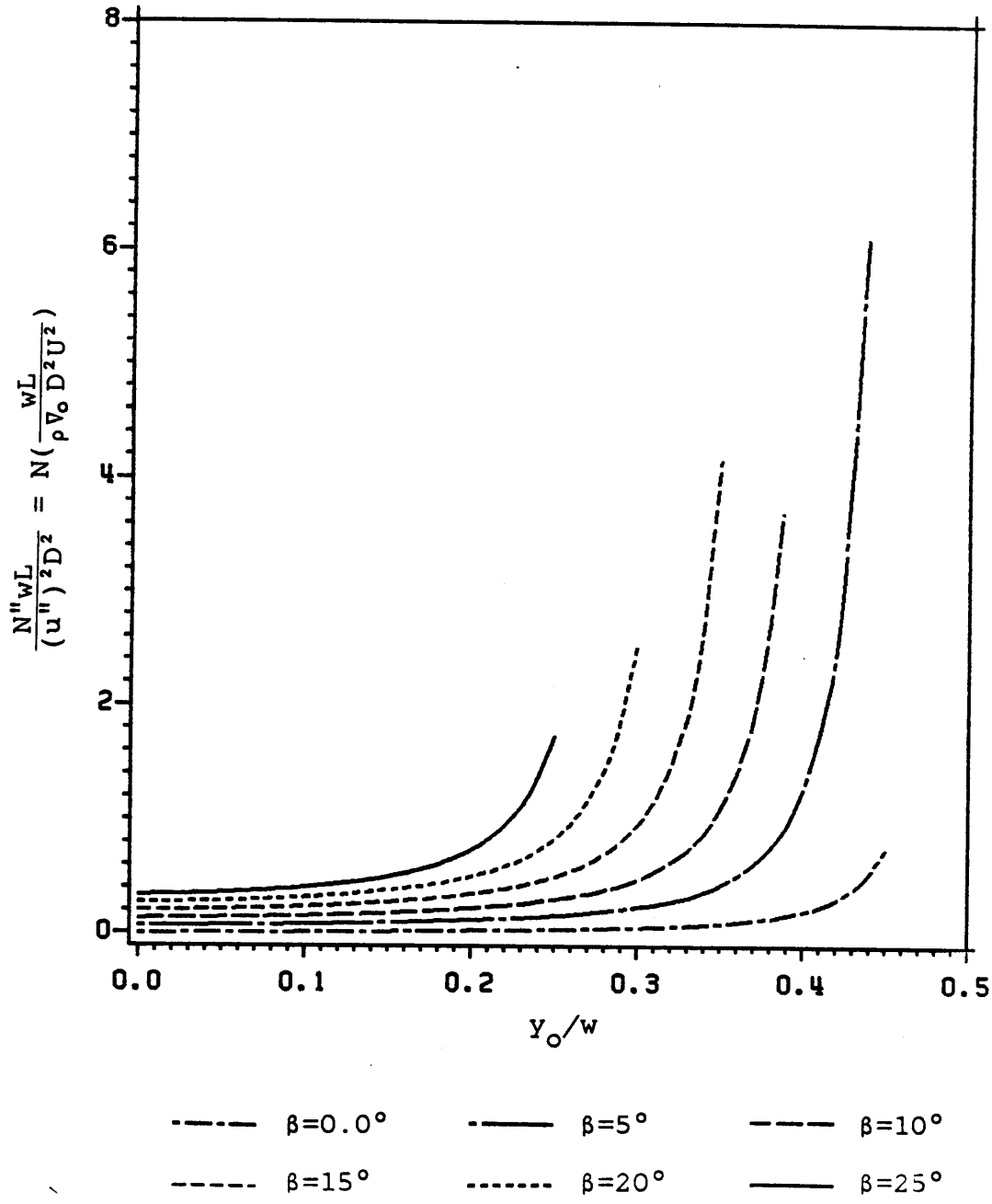

Figure 28. Variation of Moment with Lateral Position at Various Angles for a Series 60, Block .8 Hull at a Width and Depth of w/L=1 and h/w=.2.

5.0 CONCLUSIONS

In this work it was found that, although the theory gave good qualitative results for the side force when a body was parallel to a wall, it was unable to give correct predictions for either the yaw moment or the side force due to angular orientation. This demonstrates that the simple model used here is adequate for parallel orientation, but is unable to be extended into other applications. The consequence of this result is the need for a more complete representation of the hydrodynamic model for the body, which would involve additional singularity systems to correct for the induced flows arising from the images and their influence on the boundary condition on the body. Furthermore, the required analysis in that case would also include unsteady effects that have been ignored in the present study.

BIBLIOGRAPHY

1. Ashley, H., and M. Landahl, Aerodynamics of Wings and Bodies, Dover Publications, Inc., 1965.

2. Beck, R. F., "Forces and Moments on a Ship Moving in a Shallow Channel," Journal of Ship Research, Vol. 21, No. 2, June 1977, pp. 107-119.

3. Burden, R. L., J. D. Faires, and A. C. Reynolds, Numerical Analysis, 2nd Ed., Prindle, Weber, and Schmidt, 1981.

4. Cohen, S. B., and R. F. Beck, "Experimental and Theoretical Hydrodynamic Forces on a Mathematical Model in Confined Waters," Journal of Ship Research, Vol. 27, No. 2, June 1983, pp. 75-89.

5. Cummins, W. E., "The Force and Moment on a Body in a Time-Varying Potential Flow," Journal of Ship Research, Vol. 1, No. 1, April 1957, pp. 7-18.

6. Dand, I. W., "Hydrodynamic Aspects of Shallow Water Collisions," Transactions of the Royal Institute of Naval Architects, Vol. 118, 1976, pp. 323-346.

7. Hess, F., "Lateral Forces on a Ship Approaching a Vertical Wall: A Theoretical Model," Journal of Ship Research, Vol. 23, No. 4, December 1979, pp. 284-296.

8. Karamcheti, K., Principles of Ideal-Fluid Aerodynamics, Robert E. Krieger Publishing Company, 1980.

9. Liepmann, H. W., and A. Roshko, Elements of Gasdynamics, John Wiley and Sons, Inc., 1957.

10. Lunde, J. K., "On the Linearized Theory of Wave Resistance for Displacement Ships in Steady and Accelerated Motion," Transactions SNAME, 1951.

11. Newman, J. N., "Some Theories for Ship Manoeuvring," Journal of Mechanical Engineering Science, Vol. 14, No. 7, 1972, pp. 34-42.

12. Newman, J. N., Marine Hydrodynamics, The MIT Press, 1982.

13. Norrbin, N. H., "Theory and Observations on the use of a Mathematical Model for Ship Maneuvering in Deep and Confined Waters," Eighth Symposium of Naval Hydrodynamics, ACR-179 Office of Naval Research, Department of the Navy, 1970 pp. 807-904.

14. Robertson, J. M. Hydrodynamics in Theory and Application, Prentice-Hall, Inc., 1965.

15. White, F. M., Fluid Mechanics, McGraw Hill Book Company, 1979.

APPENDIX A.

COMPUTER PROGRAM FOR DETERMINING THE HYDRODYNAMIC SIDE FORCE ACTING ON A SPHEROID IN PROXIMITY OF A SINGLE WALL IN SHALLOW WATER

Definition of Program Variables

A ..... Lower limit of integration

B ..... Upper limit of integration

BETA ..... Angle in degrees between the x and x_1 axes

D ..... Body diameter

HL ..... Ratio of fluid depth to body length (h/L)

LM ..... Number of M summation to convergence for a specified criteria

Q ..... Convergence criteria

S ..... Cross sectional area

SL ..... Body length

SP ..... Derivative of the cross sectional area with respect to x

VOL ..... Volume displacement at rest

W ..... Weights for Gauss-Legendre Quadrature

X ..... Location on x_1-axis

Y ..... Resultant nondimenional side force for given YSL and HL values

YSL ..... Ratio of body center to wall distance over body length (y_s/L)

Z ..... Zeros (roots) for Gauss-Legendre Quadrature

COMPUTER PROGRAM

```
      DIMENSION HL(4),S(21),X(22),SP(20),A(21),B(21),Z(2),W(2)
      CALL TIMEON
      ATIME=0.
C
C     DETERMINATION OF THE NONDIMENSIONAL BANK SUCTION FORCE
C        ACTING ON A SPHEROID (SINGLE WALL, FINITE DEPTH)
C
C     NONDIMENSIONAL DEPTH PARAMETER H/L IS HL
C     NONDIMENSIONAL SEPARATION PARAMETER YS/L IS YSL
C
C
C        EMPLOYING A GAUSS-LEGENDRE QUADRATURE
C              FOR DOUBLE INTEGRATION
C
C     INTEGRALS WILL USE A TWO POINT QUADRATURE (L=2)
      L=2
C     ZEROS (ROOTS)
      Z(1)=.577350269189626
      Z(2)=-Z(1)
C     WEIGHTS
      W(1)=1.
      W(2)=1.
C     ANGLE BETA (DEGREES)
      BETA=0.
      WRITE(7,680)BETA
  680 FORMAT('1',/,/,/,3X,
     &'SPHEROID WITH SINGLE WALL, FINITE DEPTH',/,3X,
     &'GAUSS-LEGENDRE QUADRATURE FOR DOUBLE INTEGRATION',/,
     &3X,'ANGLE BETA =',F7.2,' DEGREES',/)
C     MAXIMUM NUMBER OF SUMMATION
      LMAX=70
C     ERROR CRITERIA
      Q=0.001
C     INPUT H/L VALUES
      HL(1)=.05
      HL(2)=.1
      HL(3)=.25
      HL(4)=1.
C     SPHEROID STARTS HERE
      PI=4.*ATAN(1.)
C     BODY LENGTH AND DIAMETER
      SL=100.
      D=14.
      D2=D*D
      X(1)=SL/2.
      XD=SL/20.
      VOL=PI*SL*D2/6.
C     CALCULATE CROSS SECTIONAL AREAS
```

```
      DO 10 J=1,21
         S(J)=PI*D2*(.25-X(J)*X(J)/(SL*SL))
         X(J+1)=X(J)-XD
   10 CONTINUE
      B(1)=SL/2
      A(1)=B(1)-XD
C     CALCULATE LIMITS OF INTEGRATION AND
C     CROSS SECTIONAL AREA DERIVATIVE
      DO 20 J=1,20
         SP(J)=(S(J)-S(J+1))/XD
         B(J+1)=A(J)
         A(J+1)=A(J)-XD
   20 CONTINUE
      BETAR=BETA*4.*ATAN(1.)/180.
      CB=COS(BETAR)
      CB2=CB*CB
      SB=SIN(BETAR)
C     CHECK TO SEE IF ANGLE WOULD MAKE SHIP TOUCH WALL
      SSB=ABS(SB)
      IF(SSB.LE..1) THEN
              BSL=0.0
         ELSE IF(SSB.LE..2) THEN
              BSL=.05
         ELSE IF(SSB.LE..3) THEN
              BSL=.1
         ELSE IF(SSB.LE..4) THEN
              BSL=.15
         ELSE IF(SSB.LE..5) THEN
              BSL=.2
         ELSE IF(SSB.LE..6) THEN
              BSL=.25
         ELSE
              BSL=.25
              WRITE(7,685)
  685         FORMAT(/,3X,'WARNING, ANGLE MAY BE EXCESSIVE ...',
     &/,3X,'CHECK RESULTS CAREFULLY!',/)
      ENDIF
      CALL TIMECK(NM)
      ATIME=NM/100.
C     DO LOOP FOR H/L VALUES
      DO 250 IH=1,4
      CALL TIMEON
      YSL=BSL+.0375
      ASL=BSL+.14999
      WRITE(7,690)HL(IH)
  690 FORMAT(3X,'NON-DIMENSIONAL FORCE FOR H/L=',F7.3,/)
      WRITE(1,695)HL(IH),BETA
  695 FORMAT(3X,'H/L=',F7.3,3X,'BETA=',F7.3)
      WRITE(7,700)
  700 FORMAT(3X,'YS/L     FORCE    # OF M SUMMATION')
  260 IF(YSL.GE.ASL) YSL=YSL+.05
```

```
      IF(YSL.LE.ASL) YSL=YSL+.0125
      YS=YSL*SL
      CON=-SL*SL*SL/(4.*PI*D2*VOL)
      Y=0
      LM=1
      M=-1
C     LOOP FOR M SUMMATION
  210 M=M+1
      E=4.*M*M*HL(IH)*HL(IH)*SL*SL
C     GAUSS-LEGENDRE QUADRATURE
      E2=0
      E3=0
      DO 30 IO=1,20
      DO 40 II=1,20
      C1=(B(IO)-A(IO))*(B(II)-A(II))/4.
      C2=A(IO)+B(IO)
      C3=A(II)+B(II)
      FUNWE2=0
      FUNWE3=0
C     OUTSIDE INTEGRAL
      DO 50 J=1,L
      R=(Z(J)*(B(II)-A(II))+C3)/2.
C     INSIDE INTEGRAL
      DO 60 I=1,L
      C=(Z(I)*(B(IO)-A(IO))+C2)/2.
      E4=R-C
      E5=R*SB-2.*YS+C*SB
      D3=E4*E4*CB2+E5*E5+E
      FUN2=E5/(D3*SQRT(D3))
      FUN3=E4/(D3*SQRT(D3))
      FUNWE2=W(I)*W(J)*FUN2+FUNWE2
      FUNWE3=W(I)*W(J)*FUN3+FUNWE3
C     INSIDE
   60 CONTINUE
C     OUTSIDE
   50 CONTINUE
      E2=E2+FUNWE2*C1*SP(IO)*SP(II)
      E3=E3+FUNWE3*C1*SP(IO)*SP(II)
   40 CONTINUE
   30 CONTINUE
      YN=Y+2.*CON*(E2*CB+E3*SB*CB)
      IF(M.EQ.0) GOTO 200
      GOTO 220
  200 Y=YN/2
      GOTO 210
C     CHECK CONVERGENCE ON M SUMMATION
  220 DIF=YN-Y
      IF(ABS(DIF/YN).LE.Q) GOTO 230
      IF(ABS(DIF).LE.Q) GOTO 230
      LM=LM+1
      IF(LM-LMAX) 240,230,230
```

```
  240 Y=YN
      GOTO 210
  230 Y=YN
C     OUTPUT REULTS
      WRITE(7,710)YSL,Y,LM
      WRITE(1,710)YSL,Y
  710 FORMAT(2X,F6.4,2X,F7.3,9X,I3)
      IF(YSL.GE..9999999) GOTO 245
      GOTO 260
  245 CALL TIMECK(NN)
      TIME=NN/100.
      ATIME=TIME+ATIME
      WRITE(7,720)TIME
  720 FORMAT(/,3X,'CPU TIME (SECONDS) =',F6.2,/)
  250 CONTINUE
      WRITE(7,740)ATIME
  740 FORMAT(3X,'TOTAL CPU TIME (SECONDS) =',F6.2,/,'1')
      STOP
      END
```

APPENDIX B.

COMPUTER PROGRAM FOR DETERMINING THE HYDRODYNAMIC YAW MOMENT ACTING ON A SERIES 60, BLOCK .80 HULL IN A CANAL IN SHALLOW WATER

Definition of Program Variables

A ..... Lower limit of integration

B ..... Upper limit of integration

BETA ..... Angle in degrees between the x and x_1 axes

D ..... Effective body diameter

HW ..... Ratio of fluid depth to canal width (h/w)

LM ..... Number of M summation to convergence for a specified criteria

Q ..... Convergence criteria

S ..... Cross sectional area

SL ..... Body length

SP ..... Derivative of the cross sectional area with respect to x

VOL ..... Volume displacement at rest

W ..... Weights for Gauss-Legendre Quadrature

WL ..... Ratio of canal width to body length (w/L)

X ..... Location on x_1-axis

YH ..... Resultant nondimenional yaw moment for given YOW, WL, and HW values

YOW ..... Ratio of body center to canal centerline distance over body length (y_o/w)

Z ..... Zeros (roots) for Gauss-Legendre Quadrature

COMPUTER PROGRAM

```
      DIMENSION Z(5),W(5),A(21),B(21),S(21),SP(20),
     &X(22),HW(4),WL(2)
      CALL TIMEON
C
C     DETERMINATION OF THE HYDRODYNAMIC MOMENT
C      ACTING ON A SERIES 60, BLOCK .80 HULL
C            AT AN ANGLE IN A CANAL
C
C     NON-DIMENSIONAL DEPTH PARAMETER H/W IS HW
C     NON-DIMENSIONAL SEPARATION PARAMETER YO/W IS YOW
C     NON-DIMENSIONAL WIDTH PARAMETER W/L IS WL
C
C           EMPLOYING A GAUSS-LEGENDRE QUADRATURE
C                 FOR DOUBLE INTEGRATION
C
C     INPUT ANGLE BETA
      BETA=25.
      WRITE(11,680)BETA
  680 FORMAT(/,/,/,3X,
     &'SERIES 60, BLOCK .80 HULL IN A CANAL AT AN ANGLE',/,3X
     &,'GAUSS-LEGENDRE QUADRATURE FOR DOUBLE INTEGRATION',/,
     &3X,'ANGLE BETA =',F7.2,' DEGREES',/)
C     INTEGRALS WILL USE A FIVE POINT QUADRATURE (L=5)
      L=5
C     ZEROS (ROOTS)
      Z(1)=0.
      Z(2)=.538469310105683
      Z(3)=-Z(2)
      Z(4)=.906179845938664
      Z(5)=-Z(4)
C     WEIGHTS
      W(1)=.568888888888889
      W(2)=.478628670499366
      W(3)=W(2)
      W(4)=.236926885056189
      W(5)=W(4)
C     MAXIMUM NUMBER OF SUMMATION
      MAX=70
C     ERROR CRITERIA
      Q=.001
C     INPUT H/W VALUES
```

```
      HW(1)=.2
      HW(2)=.4
      HW(3)=2.
      HW(4)=20.
C     INPUT W/L VALUES
      WL(1)=.5
      WL(2)=1.
C     SHIP STARTS HERE
C     OBJECT PARAMETERS
      PI=4.*ATAN(1.)
C     BODY LENGTH
      SL=193.
C     EFFECTIVE DIAMETER
      D=27.744
      D2=D*D
      X(1)=SL/2.
      XD=SL/20.
C     CROSS SECTIONAL AREA
      S(1)=0.
      S(2)=276.8106
      S(3)=451.2311
      S(4)=544.7236
      S(5)=589.3064
      S(6)=602.7205
      DO 10 I=7,12
      S(I)=604.5450
   10 CONTINUE
      S(13)=603.9368
      S(14)=601.5041
      S(15)=588.7320
      S(16)=553.4422
      S(17)=486.9732
      S(18)=392.2859
      S(19)=271.5147
      S(20)=128.2024
      S(21)=5.1421
      VOL=96252.8
      B(1)=SL/2.
      A(1)=B(1)-XD
C     CALCULATE LIMITS OF INTEGRATION AND
C     CROSS SECTIONAL AREA DERIVATIVE
      DO 20 J=1,20
      SP(J)=(S(J)-S(J+1))/XD
      B(J+1)=A(J)
      A(J+1)=A(J)-XD
   20 CONTINUE
      BETAR=BETA*4*ATAN(1.0)/180
      CB=COS(BETAR)
      CB2=CB*CB
      SB=SIN(BETAR)
      CALL TIMECK(NM)
```

```
      ATIME=NM/100.
C     START LOOPS FOR H/W, W/L
      DO 320 JJ=1,2
      DO 310 IH=1,4
      CALL TIMEON
      IF(JJ.EQ.2) HW(IH)=HW(IH)/2.
      WRITE(11,690)WL(JJ),HW(IH)
  690 FORMAT(3X,'NON-DIMENSIONAL MOMENT FOR W/L=',F5.2,
     &3X,'H/W=',F6.2,/)
      WRITE(1,695)WL(JJ),HW(IH)
  695 FORMAT(3X,'W/L=',F5.2,3X,'H/W=',F6.2)
      WRITE(11,700)
  700 FORMAT(3X,'YO/W',4X,'MOMENT   # OF M SUMMATION')
C     CHECK TO SEE IF ANGLE WOULD CAUSE 'SHIP' TO CONTACT WALL
      XW=SB/(2.*WL(JJ))
      XW=ABS(XW)
      IF(XW.GE..5) THEN
         WRITE(11,710)
  710    FORMAT(/,5X,'ANGLE TO GREAT, CONTACT WITH WALL',/)
         GOTO 320
      ELSE
         CONTINUE
      END IF
      YOWM=.5-XW
      IF(YOWM.LE..05) THEN
           CYOW=-1.
        ELSE IF(YOWM.LE..10) THEN
           CYOW=.0499
        ELSE IF(YOWM.LE..15) THEN
           CYOW=.0999
        ELSE IF(YOWM.LE..20) THEN
           CYOW=.1499
        ELSE IF(YOWM.LE..25) THEN
           CYOW=.1999
        ELSE IF(YOWM.LE..30) THEN
           CYOW=.2499
        ELSE IF(YOWM.LE..35) THEN
           CYOW=.2999
        ELSE IF(YOWM.LE..40) THEN
           CYOW=.3499
        ELSE IF(YOWM.LE..45) THEN
           CYOW=.3999
        ELSE
           CYOW=.4499
      END IF
      WC=WL(JJ)*SL
      H=HW(IH)*WC
      CON=-WC*SL/(4.*PI*D2*VOL)
      YOW=-.05
C     START OF YO/W LOOP
      G1=CYOW-.05
```

```
      G2=CYOW-.1
  200 IF(YOW.GE.G1) YOW=YOW+.0125
      IF(YOW.LE.G1) YOW=YOW+.025
      IF(YOW.LE.G2) YOW=YOW+.025
      YO=YOW*WC
      LM=1
      M=-1
C     LOOP FOR M SUMMATION
  210 M=M+1
      E=4.*M*M*H*H
      K=0
      Y=0.
      N=-1
C     LOOP FOR N SUMMATION
  110 N=N+1
      PM=(-1)**N
C     GAUSS-LEGENDRE QUADRATURE
      E2=0.
      E3=0.
      DO 30 IO=1,20
      DO 40 II=1,20
      C1=(B(IO)-A(IO))*(B(II)-A(II))/4.
      C2=A(IO)+B(IO)
      C3=A(II)+B(II)
      FUNWE2=0
      FUNWE3=0
C     OUTSIDE INTEGRAL
      DO 50 J=1,L
      R=(Z(J)*(B(II)-A(II))+C3)/2.
C     INSIDE INTEGRAL
      DO 60 I=1,L
      C=(Z(I)*(B(IO)-A(IO))+C2)/2.
      E4=R-C
      E5=YO+R*SB+N*WC-PM*(YO+C*SB)
      D1=E4*E4*CB2+E5*E5+E
      FUNC2=E5*R/(D1*SQRT(D1))
      FUNC3=E4*R/(D1*SQRT(D1))
      FUNWE2=W(I)*W(J)*FUNC2+FUNWE2
      FUNWE3=W(I)*W(J)*FUNC3+FUNWE3
C     INSIDE
   60 CONTINUE
C     OUTSIDE
   50 CONTINUE
      E2=E2+FUNWE2*C1*SP(II)*SP(IO)
      E3=E3+FUNWE3*C1*SP(II)*SP(IO)
   40 CONTINUE
   30 CONTINUE
      HOLD=CON*(E2*CB+E3*CB*SB)
      IF(N.EQ.0) THEN
              Y=HOLD
              GOTO 110
```

```
         ELSE
              CONTINUE
       ENDIF
       N=-N
C      GAUSS-LEGENDRE QUADRATURE
       E2=0
       E3=0
       DO 70 IO=1,20
       DO 80 II=1,20
       C1=(B(IO)-A(IO))*(B(II)-A(II))/4.
       C2=A(IO)+B(IO)
       C3=A(II)+B(II)
       FUNWE2=0
       FUNWE3=0
C      OUTSIDE INTEGRAL
       DO 90 J=1,L
       R=(Z(J)*(B(II)-A(II))+C3)/2.
C      INSIDE INTEGRAL
       DO 100 I=1,L
       C=(Z(I)*(B(IO)-A(IO))+C2)/2.
       E4=R-C
       E5=YO+R*SB+N*WC-PM*(YO+C*SB)
       D1=E4*E4*CB2+E5*E5+E
       FUNC2=E5*R/(D1*SQRT(D1))
       FUNC3=E4*R/(D1*SQRT(D1))
       FUNWE2=W(I)*W(J)*FUNC2+FUNWE2
       FUNWE3=W(I)*W(J)*FUNC3+FUNWE3
C      INSIDE
  100  CONTINUE
C      OUTSIDE
   90  CONTINUE
       E2=E2+FUNWE2*C1*SP(II)*SP(IO)
       E3=E3+FUNWE3*C1*SP(II)*SP(IO)
   80  CONTINUE
   70  CONTINUE
       E9=CON*(E2*CB+E3*CB*SB)
       YN=Y+HOLD+E9
C      CHECK CONVERGENCE ON N LOOP
       DIF=YN-Y
       IF(YN.EQ.0) GOTO 120
       IF(ABS(DIF/YN).LE.Q) GOTO 130
  120  IF(ABS(DIF).LE.Q) GOTO 130
       K=K+1
       IF(K-MAX) 140,130,130
  140  Y=YN
       N=-N
       GOTO 110
  130  IF(M.EQ.0) THEN
          YH=YN
          GOTO 210
       ENDIF
```

```
      YHN=2.*YN+YH
C     CHECK CONVERGENCE ON M LOOP
      DIFF=YHN-YH
      IF(YHN.EQ.0) GOTO 150
      IF(ABS(DIFF/YHN).LE.Q) GOTO 160
  150 IF(ABS(DIFF).LE.Q) GOTO 160
      LM=LM+1
      IF(LM-MAX) 170,160,160
  170 YH=YHN
      GOTO 210
C     OUTPUT RESULTS
  160 WRITE(11,720)YOW,YH,LM
      WRITE(1,720)YOW,YH
  720 FORMAT(1X,F7.4,1X,F8.3,9X,I3)
  340 IF(YOW.GE.CYOW) GOTO 300
      GOTO 200
  300 CALL TIMECK(NN)
      TIME=NN/100.
      ATIME=ATIME+TIME
      WRITE(11,730)TIME
  730 FORMAT(/,3X,'CPU TIME (IN SECONDS) =',F6.2,/)
  310 CONTINUE
  320 CONTINUE
      WRITE(11,750)ATIME
  750 FORMAT(3X,'TOTAL CPU TIME (IN SECONDS) =',F6.2,/)
      STOP
      END
```

The vita has been removed from the scanned document